Supplementary Figure S1

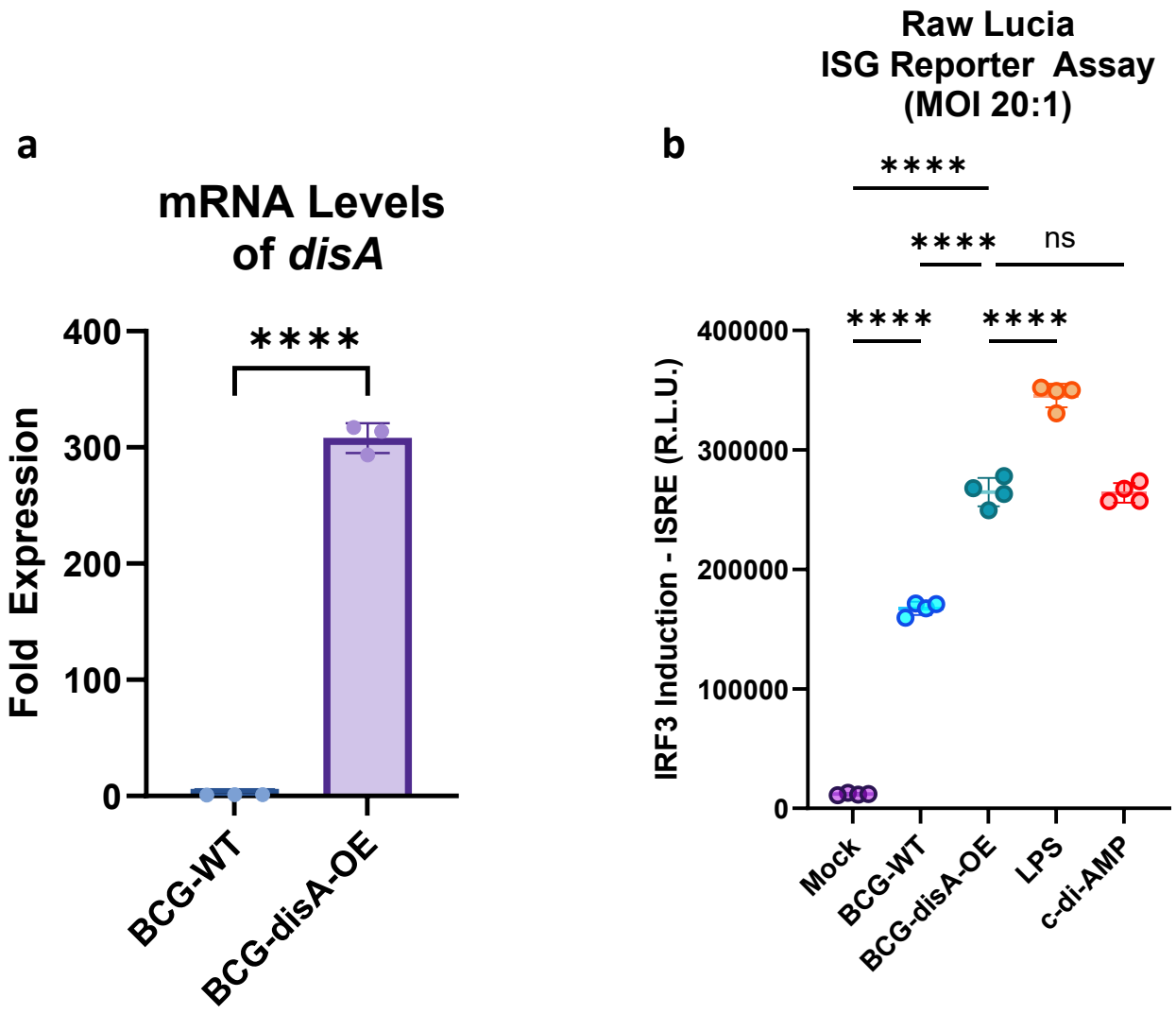

Supplementary Figure S1. Validation of *disA* overexpression in BCG-*disA*-OE and induction of IRF3 signaling. a. mRNA levels of *disA* in log-phase BCG cultures relative to *M. tuberculosis sigA* (Rv2703) (n=3 independent biological replicates). **b**. IRF3 induction measured in RAW-Lucia ISG reporter macrophages. IRF3 induction was quantified using culture supernatants of macrophages infected at an MOI of 20:1 for 24 hrs (n=4 independent biological replicates). Data reflect means values ± SD. Statistical analyses done using 2-tailed student's T-test in panel **a**; one-way ANOVA w/Tukey's test for multiple comparisons in panel **b** (**** $p < 0.0001$).

Supplementary Figure S2

a

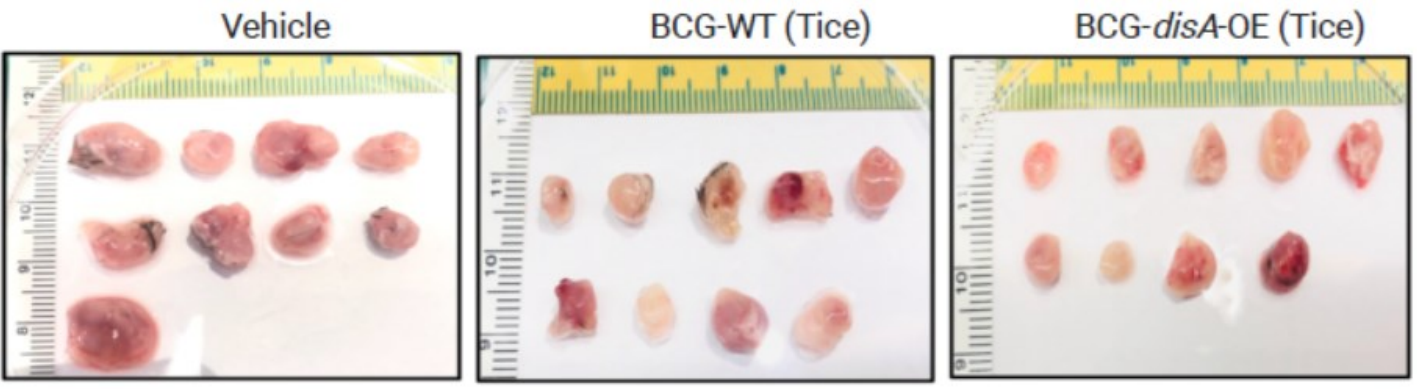

b

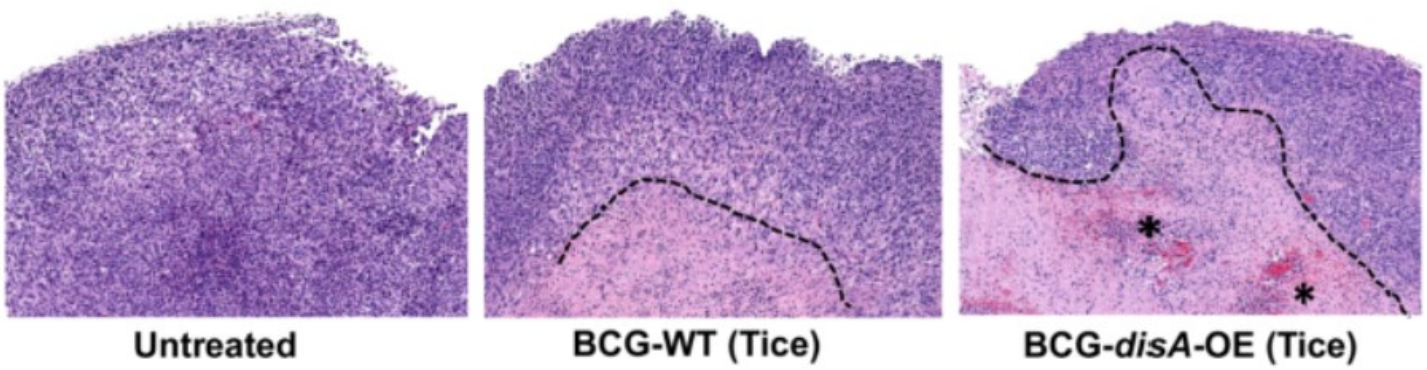

Supplementary Figure S2. BCG-*disA*-OE causes reduced tumor growth and greater tumor-associated necrosis in the heterotopic syngeneic MB49 mouse model of urothelial cancer. **a.** Tumors at necropsy on day 21 (n=9 animals/group). **b.** Representative H & E staining showing necrotic area and congestion in MB49 tumors. Similar observations were made in randomly selected 3 (n=3) tumor tissue slides per group. Untreated group shows densely packed tumor cells; BCG-WT (Tice) tumor cells with moderate necrosis (below dashed line), BCG-*disA*-OE (Tice) with extensive necrosis (below dashed line) and congestion (*). (Related to **Fig. 3a-b**).

Supplementary Figure S3

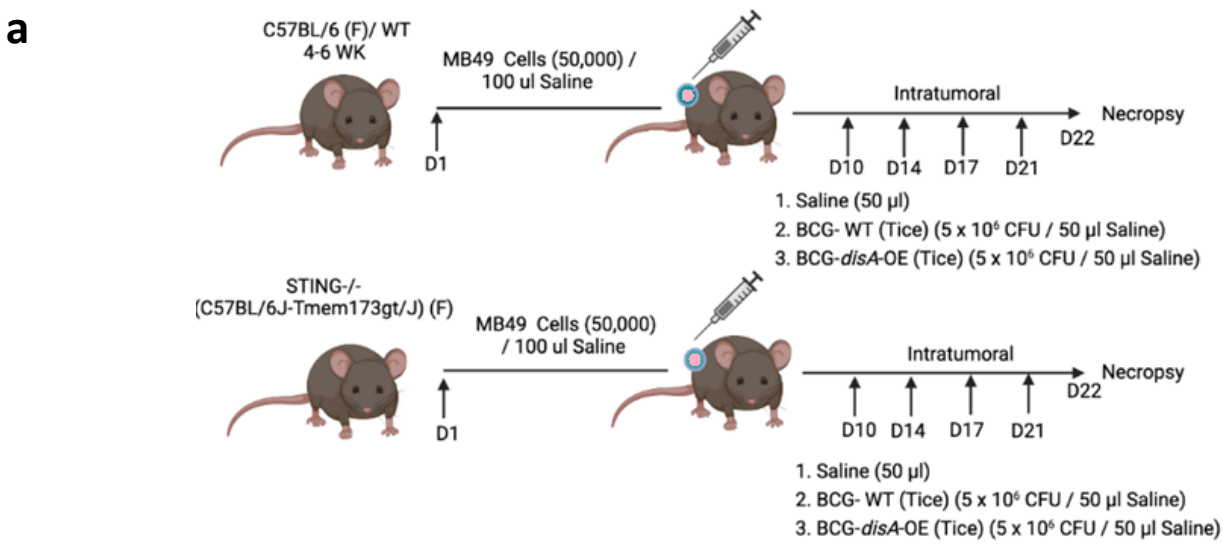

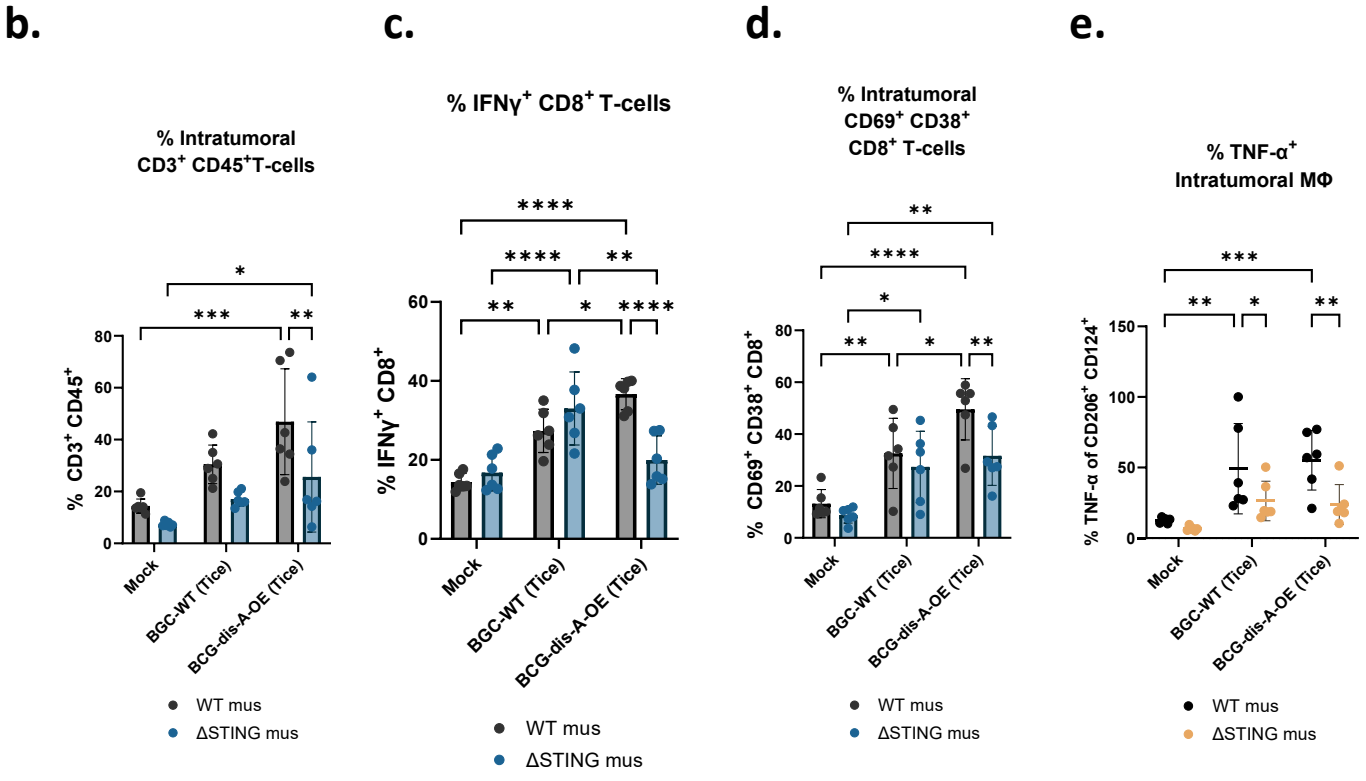

Supplementary Figure S3. **Improved antitumor efficacy of BCG-*disA*-OE is associated with differential recruitment of T cells and macrophages to tumors and is STING-dependent in the MB49 model** **a.** Schematic diagram of the MB49 syngeneic mouse model of urothelial tumors used in this experiment. **b.** Total $CD3^+$ T cells of all CD45+ leucocytes in tumors. **c.** $IFN\gamma^+$ tumor-infiltrating $CD8^+$ T cells. **d.** activated $CD8^+$ T cells (percent CD69+ CD38+ of CD8+). **e.** TNF^+-expressing immunosuppressive macrophages (percent TNFα+ of CD206+ CD124+ F4/80+ CD11b+) in MB49 tumors after necropsy. Data are presented as mean values ± S.D. (n=6 animals/group). Statistical analyses done using two-way ANOVA with Tukey's test for multiple comparisons. (* $p < 0.05$, ** $p < 0.01$, ***$p < 0.001$, **** $p < 0.0001$).

Supplementary Figure S4

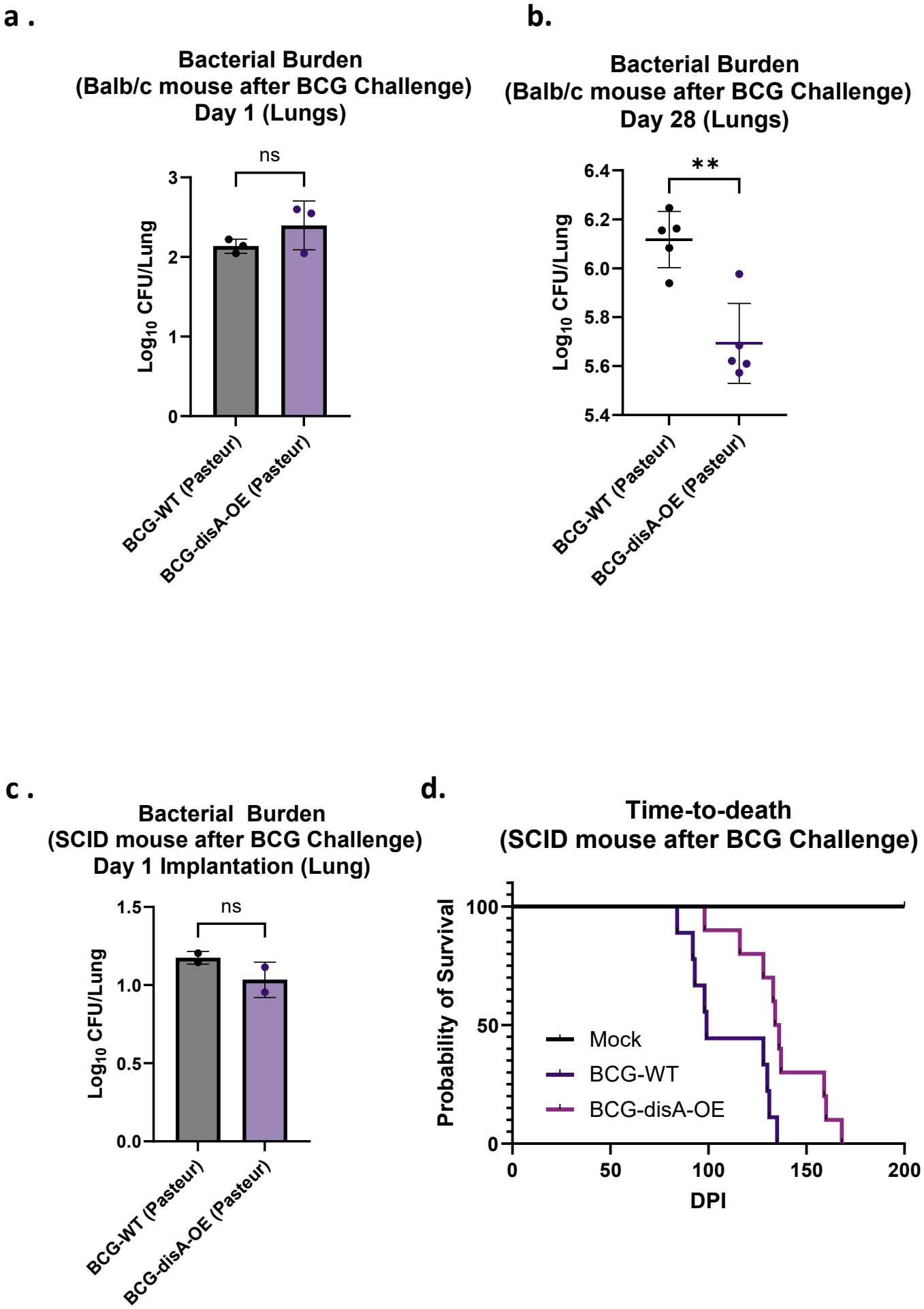

Supplementary Figure S4. BCG-*disA*-OE (Pasteur) is less pathogenic that BCG-WT in two mouse models. a. Using the same experimental scheme shown in Fig. 7a, BALB/c mice were aerosol infected and lung colony forming unit (CFU) counts at day 1 are shown (n=3 animals/group). **b.** Lung CFU counts for BALB/c mice at day 28 (n=5 animals/group). **c.** Using the same experimental scheme shown in Fig. 7c, SCID mice were aerosol infected and lung colony forming unit (CFU) counts at day 1 (n = 2 animals/group). **d**. Survival of SCID mice following low dose challenge (n=10 animals/group). The experiment was performed with BCG strains in the Pasteur background. Similar results were obtained with strains in the Tice background as shown in **Fig. 4**. Data are presented as mean values ± S.D. Statistical analyses done using 2-tailed Student's t-test (** $p < 0.01$).

Supplementary Figure S5

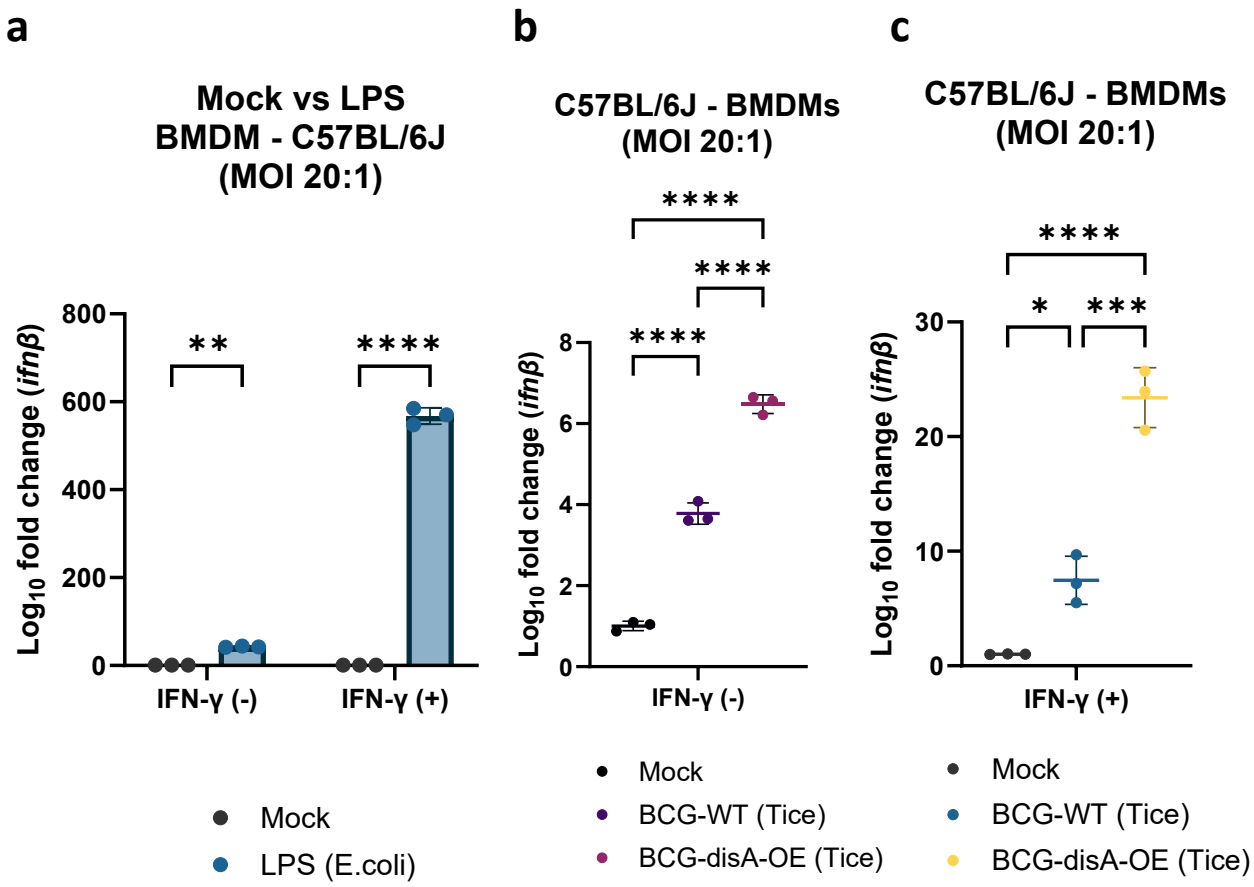

Supplementary Figure S5. BCG-*disA*-OE elicits stronger IFN-β responses than BCG-WT in murine bone marrow-derived macrophages (BMDM). a. IFN-β levels in resting and IFN-γ primed BMDMs (n=3 biological replicates). IFN-β levels were measured by RT-qPCR after a 6 hr exposure at a MOI of 20:1. Data are presented as mean values ± S.D. Gene expression analyses for cytokines and chemokines were performed 6 hr post-exposure. Statistical analyses performed using two-way (**Fig. S5a**) and one-way (**Fig. S2b-c**) ANOVA w/Tukey's multiple comparisons test in panel **a** (* $p < 0.05$, ** $p < 0.01$, ***$p < 0.001$, **** $p < 0.0001$).

Supplementary Figure S6

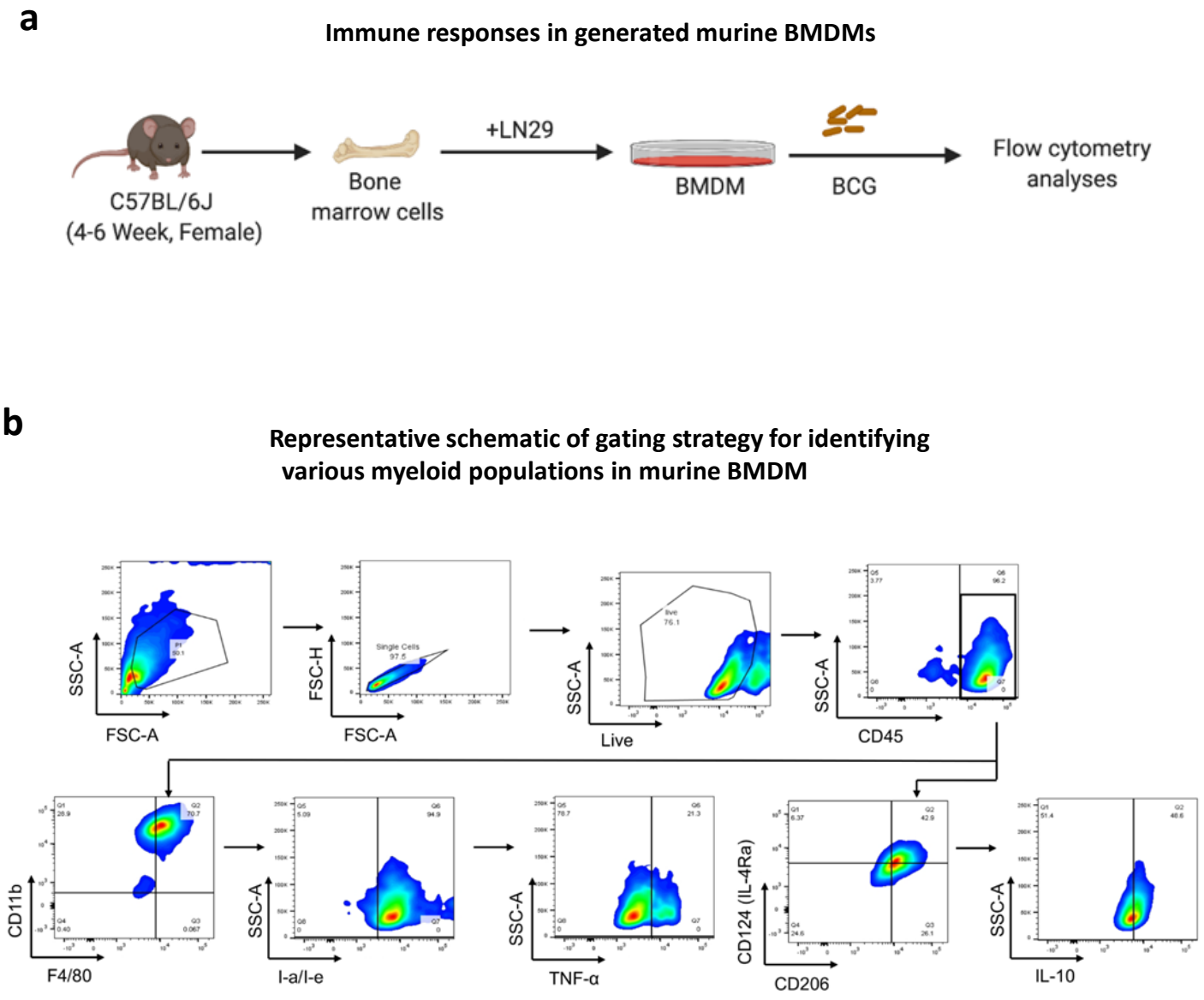

Supplementary Figure S6. Representative schematic of gating strategy to identify various myeloid populations in murine BMDMs. a. Schematic of generation of BMDMs**. b.** Representative gating scheme for identification of different myeloid cells. Briefly, leukocyte lineage was selected by gating SSC-A against $CD45^+$ populations on live cells. $CD11b^+F4/80^+$ macrophages were identified out of $CD45^+$ population. $CD11b^+F4/80^+$ macrophages were divided into MHC class II (I-a/I-e) and CD124+CD206+ populations. Expression of TNFα (M1-like macrophages) and IL-10 (M2-like macrophages) were determined on MHC class II subsets and $CD124^+CD206^+$ subsets respectively. (Related to Fig. **6a-e**).

Supplementary Figure S7

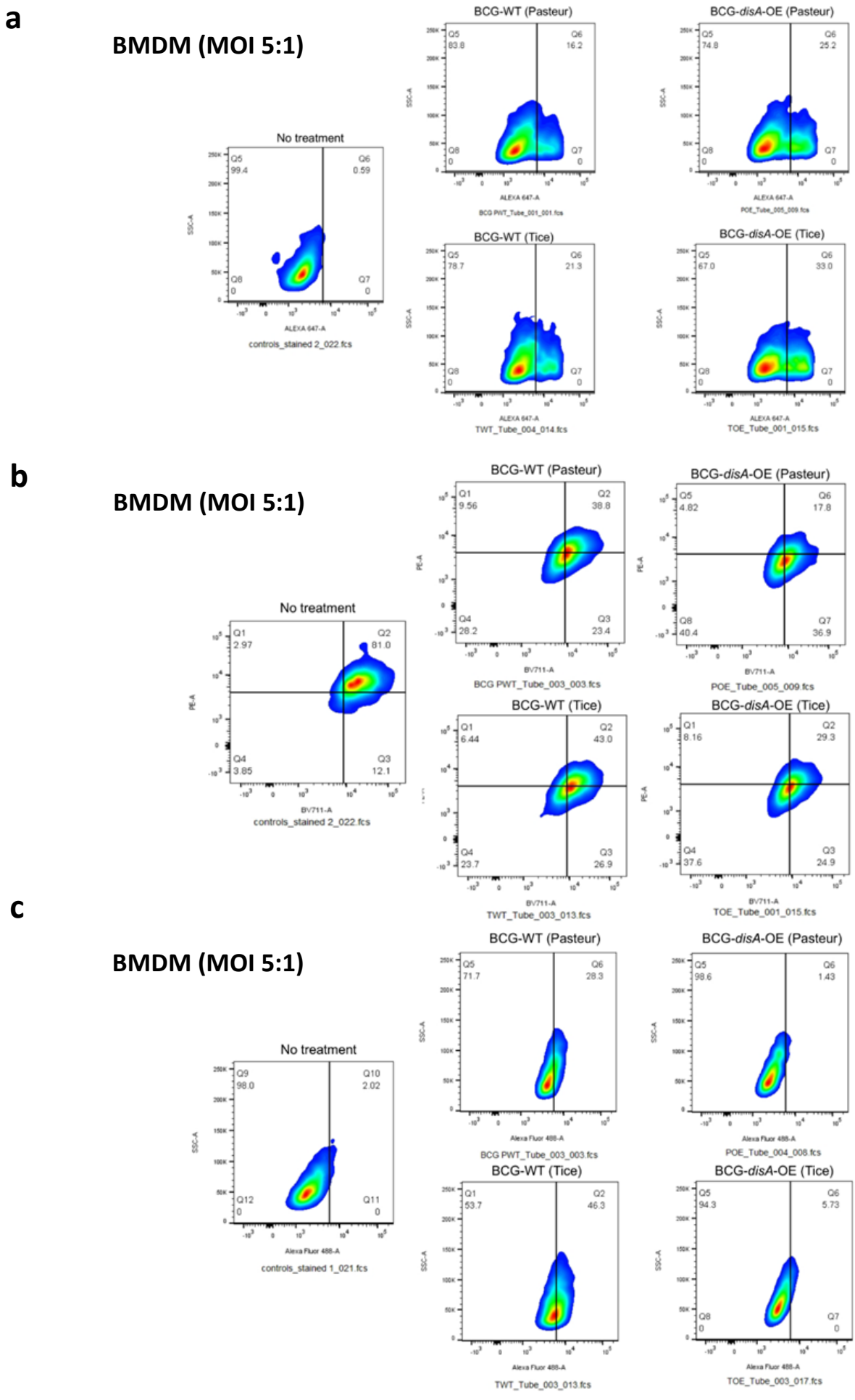

Supplementary Figure S7. BCG-*disA*-OE induces macrophage reprogramming and favors a stronger inflammatory macrophage shift in murine BMDMs. **a.** Representative FACS plots for TNF-a^{+} M1-like macrophages (MHC Class II^{+}CD11b^{+}F4/80$^{+)}$ corresponding to **Fig. 6a**. **b.** Representative FACS plots for M2-like macrophages (CD206^{+}CD124^{+}) corresponding to **Fig. 6b**. representative FACS plots. **c.** Representative FACS plots for IL-10^{+} M2-like macrophages (CD206^{+}CD124^{+}) corresponding to **Fig. 6c**.

Supplementary Figure S8

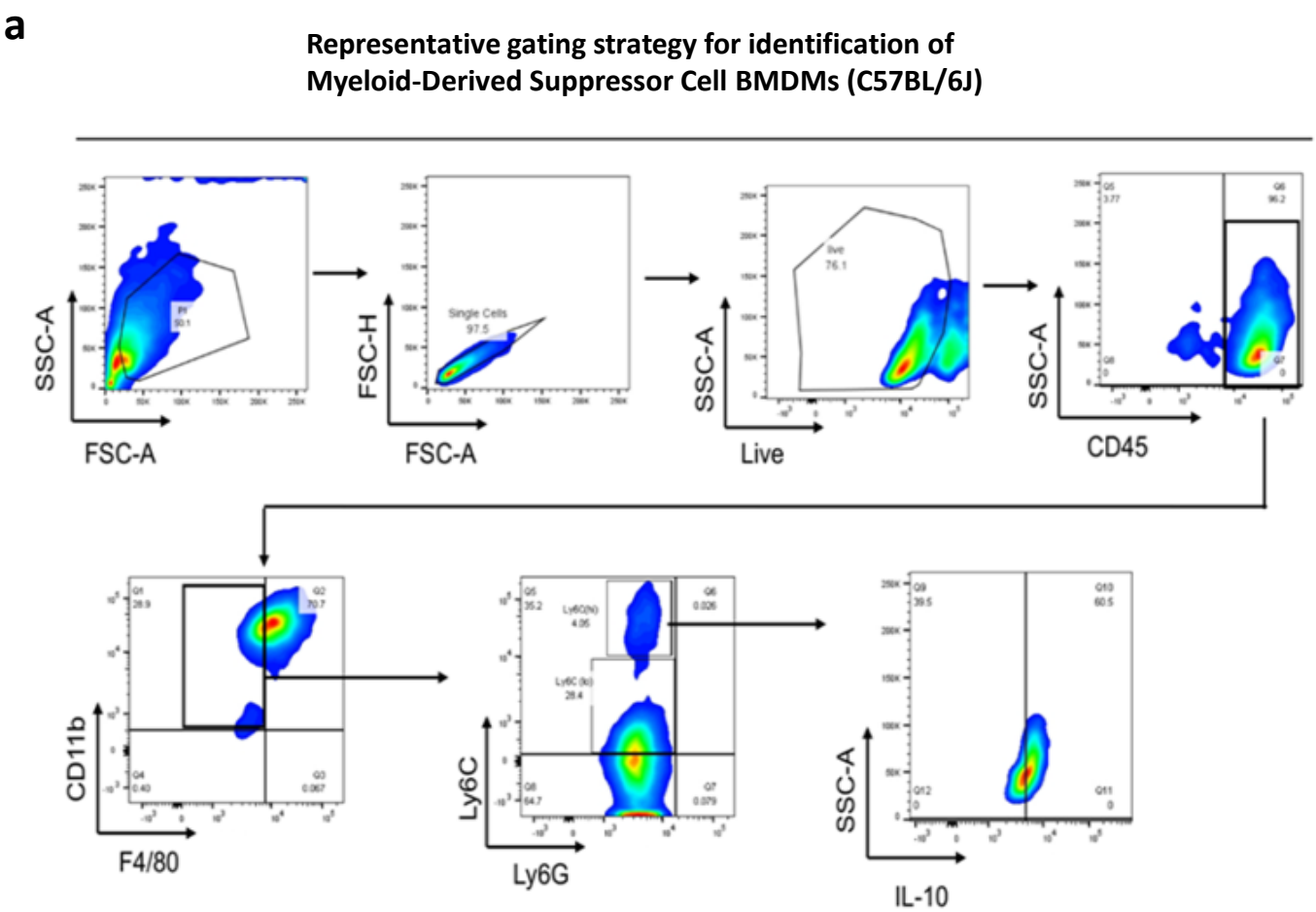

Supplementary Figure S8. Gating scheme showing identification of myeloid-derived suppressor cell populations in primary mouse macrophages after BCG exposure. Leukocyte lineage was determined on live cells by gating SSC-A against CD45+ myeloid cells. Myeloid cells were differentiated into $CD11b^{+}F4/80^{+}$ macrophages out of which $CD11b^{+}F4/80^{-}$ myeloid population was divided into Ly6C and Ly6G. Next, the $Ly6C^{(hi)}Ly6G^{-}$ immunosuppressive myeloid-derived suppressor cell populations were looked for IL-10 positivity (Related to **Fig. 6d-e**).

Supplementary Figure S9

a

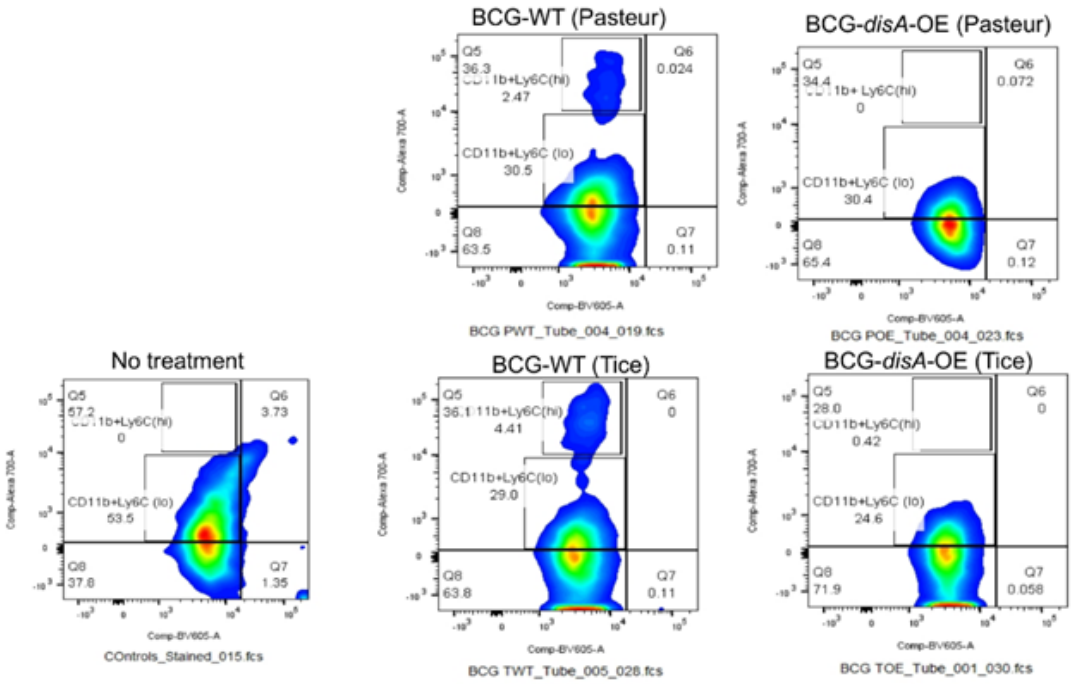

b

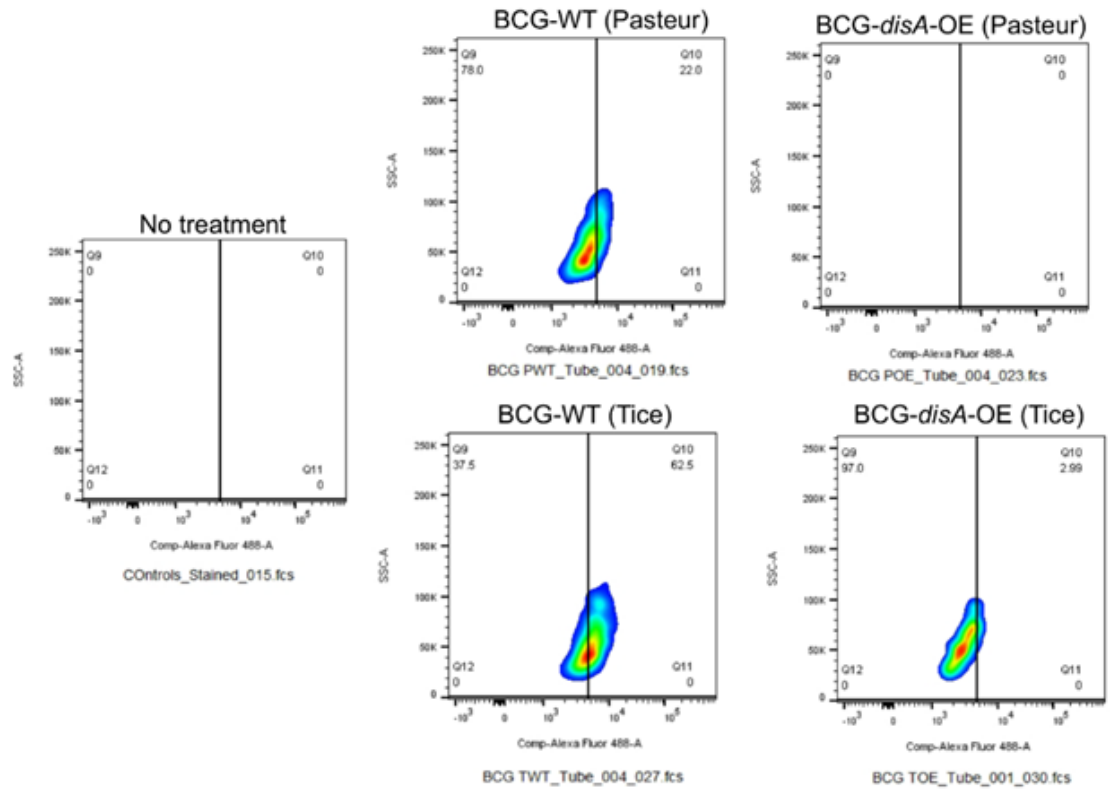

Supplementary Figure S9. Immunosuppressive monocytic-MDSCs (M-MDSCs) populations murine primary macrophages after BCG exposure. a. Representative FACS plots for M-MDSC measurements corresponding to **Fig. 6d**. **b.** Representative FACS plots for IL-10^{+} expressing M-MDSCs corresponding to **Fig. 6e**.

Supplementary Figure S10

a

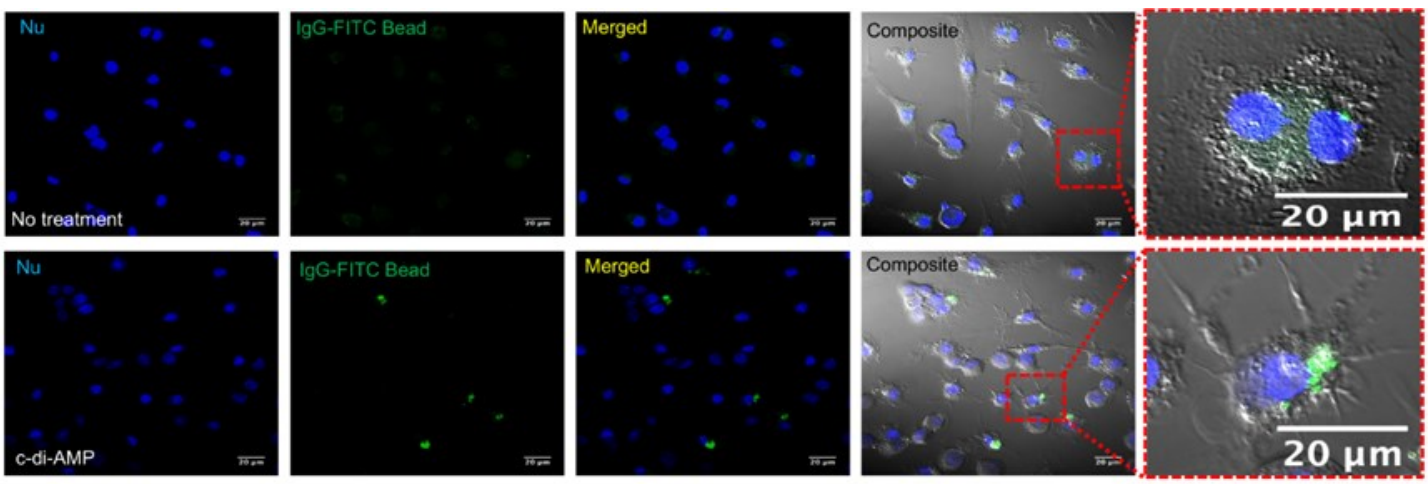

Supplementary Figure S10. The STING agonist c-di-AMP causes induction of macrophage activation. Human macrophages were transfected with c-di-AMP for 24 h and phagocytosis of FITC-labeled IgG opsonized latex beads (green) was visualized using confocal microscopy on live cells. Hoechst was used for nuclear staining (blue). Images were acquired using LSM700 confocal microscope at 63X magnification. Images were process using Fiji software. Similar results were observed across two (n=2) independent biological replicate experiments.

Supplementary Figure S11

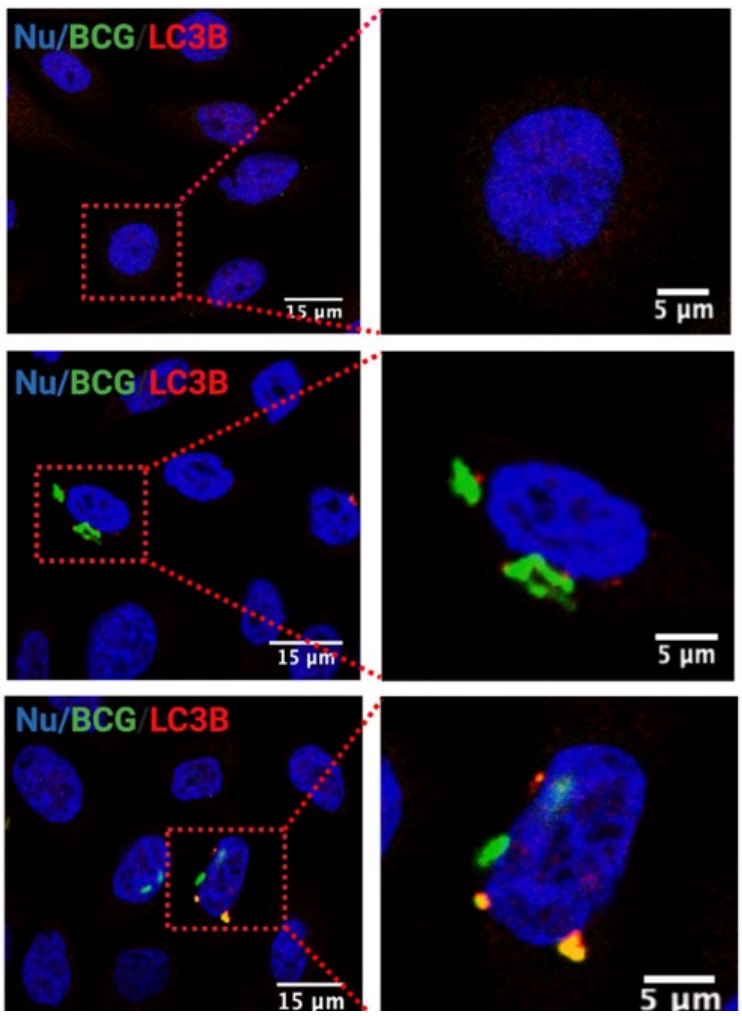

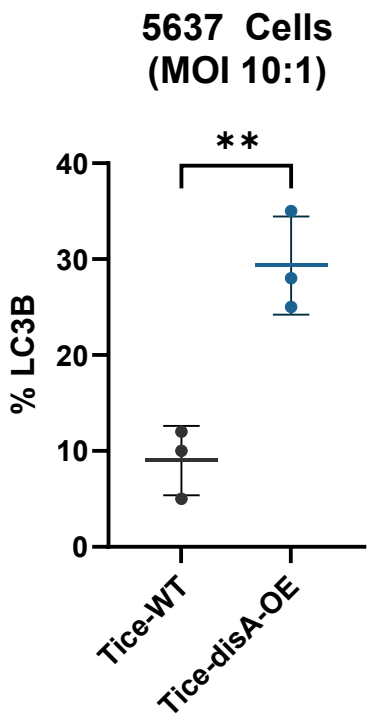

Supplementary Figure S11. BCG-*disA*-OE elicits greater autophagy induction than BCG-WT in 5637 human urothelial carcinoma cells. Autophagy induction in the 5637 human urothelial carcinoma cells in representative confocal photomicrographs. Co-localization of FITC-labeled BCG strains (green), LC3B autophagic puncta (red) appears in yellow; nuclei are blue. Quantification of co-localized BCG and LC3b puncta is shown at right. Cells were fixed using 4% paraformaldehyde 3h after infection (MOI 10:1), and images obtained with an LSM700 confocal microscope and Fiji software processing. Statistical analyses done using 2-tailed Student's t-test (** $p < 0.01$). Data shown are for BCG strains in the Tice background.

Supplementary Figure S12

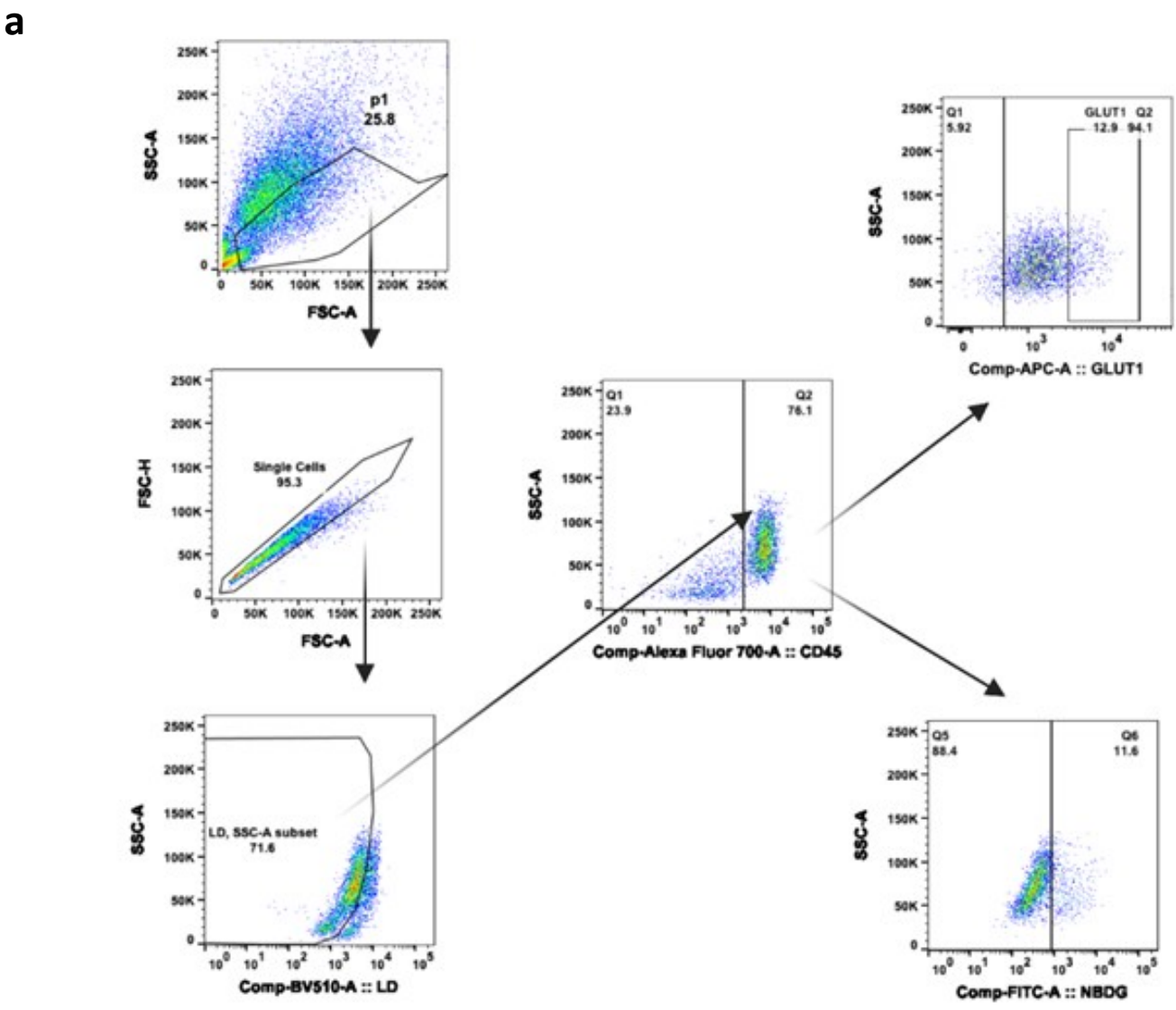

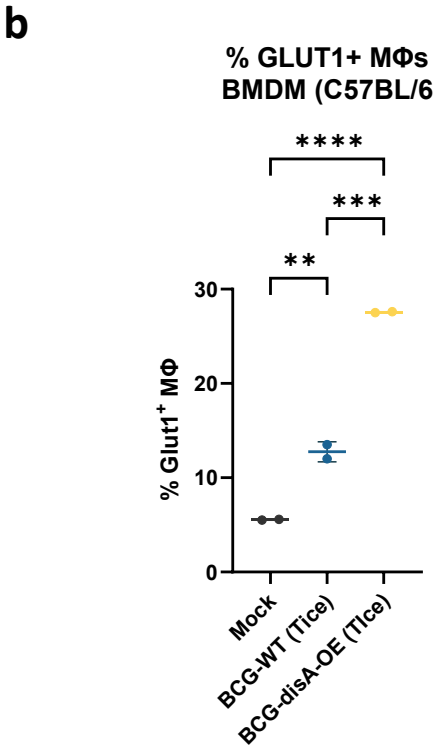

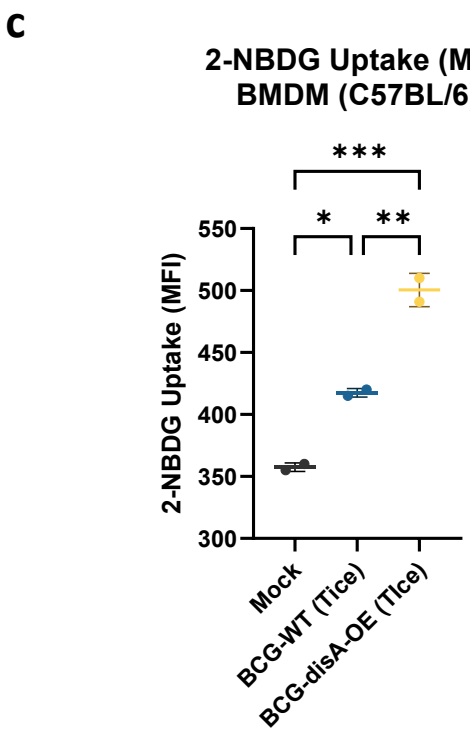

Supplementary Figure S12. BCG induced differential glucose uptake in bone-marrow-derived macrophages (BMDMs). (a) Experimental layout showing the strategy employed to determine intracellular uptake of fluorescent glucose. Briefly macrophages were infected at an MOI of 20:1 (BCG to macrophage ratio) in the presence of glucose-free medium followed by exogenous addition of 2-(*N*-(7-Nitrobenz-2-oxa-1,3-diazol-4-yl)Amino)-2-Deoxyglucose (2-NBDG). Macrophages were subsequently stained for GLUT1 and were investigated using flow cytometry. **(b-c)** Bar diagram showing induced expression of GLUT1 and intracellular fluorescent 2-NBDG in BMDMs following infection by BCG strains. Data are presented as mean values ± S.D. (n=2 independent biological replicate experiments). Data analyses were carried out using FACSDiva (v 9.0), Flowjo (v 10) and Graphpad Prism software (v 10.0.3). Statistical analysis employed a one-way ANOVA with Tukey's test for multiple comparisons (* $p < 0.05$, ** $p < 0.01$, ***$p < 0.001$, **** $p < 0.0001$).

Supplementary Table. S1: List of bacterial strains, cell lines, plasmids and antibodies used in the study

Name	Description/Source
Bacterial strains	
***M. tuberculosis* strain**	
Mtb-CDC1551	Wild-type *M. tuberculosis*
***M. bovis* BCG strains**	
BCG Pasteur	*M. bovis* BCG Pasteur
BCG-*disA*-OE (Pasteur)	BCG Pasteur strain overexpressing *disA* (MT3692) of *M.tb*
BCG Tice	*M. bovis* BCG Tice
BCG-*disA*-OE (Tice)	BCG Tice strain overexpressing *disA* (MT3692) of *M.tb*
***E. coli* strain**	
DH5-α	Competent *E. coli* (High Efficiency)
Cell lines	
Urinary bladder carcinoma cells	
RT4 (ATCC ® HTB-2™)	Human low grade urothelial cancer
5637 (ATCC® HTB-9™)	Human high-grade urothelial cancer
NBT-II (ATCC® CRL-1655™)	N-butyl-N-(4-hydroxybutyl) nitrosamine induced tumor cell line in Rattus norvegicus Nara Bladder Tumor No. 2
MB49 (Cat. SSC148, EMD Millipore)	DMBA [7,12-dimethylbenz[a]anthracene] induced murine urothelial carcinoma cells,
UPPL-1595	Luminal cell line established from a spontaneous primary bladder tumor in an Uroplakin-Cre driven PTEN/P53 knockout genetically engineered mouse model
BBN 975	Basal- cell line established from 0.05% N-Butyl-N-(4-hydroxybutyl) nitrosamine (BBN) induced murine urothelial cancer model
J28 (ATCC® HTB-1™)	high grade urothelial cancer
Reporter cells	
RAW-Lucia ISG (InvivoGen)	IFN Reporter Raw 264.7 murine macrophages
Macrophage cell lines	

J774A.1 (ATCC® TIB67™)	Murine macrophage cell line		
Plasmids			
pSD5.hsp60	Mycobacterial expression plasmid with hsp60 promoter		
pSD5hsp60.MT3692	*disA* over-expression plasmid		
Confocal Microscopy Reagents			
Primary Antibodies			
Name	**Source**	**#Cat.**	**Dilution**
LC3B	Novus Biologicals	NB100-2220	1:200
P62/SQSTM1	Sigma-Aldrich	P0067	1:100
Secondary Antibodies			
Goat anti-Rabbit IgG Alexa Fluor Plus 647	Thermo Fisher Scientific	A32733	1:1000
Chemicals/Probes			
Fluorescein 5(6)-isothiocyanate (FITC)	Sigma-Aldrich	46950	
Hoechst 33342	Thermo Fisher Scientific	62249	
Flow Cytometry Reagents			
Antibodies (mouse BMDM study)			
anti-CD45 (clone 30-F11)	Biolegend	103128	1:200
anti-CD124 (I clone 015F8)	Biolegend	144804	1:50
anti-I-A/I-E (clone M5/114.15.2)	Biolegend	107645	1:200
anti-Ly6C (clone HK1.4)	Biolegend	128046	1:50
anti-CD11b (clone M1/70)	Biolegend	101206	1:200
anti-F4/80 (clone BM8)	Biolegend	123147	1:50
anti-Ly6G (clone 1A8)	Biolegend	127641	1:100
anti CD206 (clone C068C2)	Biolegend	141721	1:200
anti-TNF (clone MP6-XT22)	Biolegend	506341	1:100
anti- IL-10 (clone JES5-16E3)	eBioscience	505021	1:50

Anti-Glut1 (clone EPR3915)	Abcam	ab195020	1:50
Antibodies (HMDM study)			
anti-CD16 (clone 3G8)	Biolegend	302028	1:50
anti-CD14 (clone 63D3)	Biolegend	367113	1:50
anti-HLA-DR (clone L243)	Biolegend	307615	1:50
anti-CD11b (clone ICRF44)	Biolegend	301351	1:100
anti-TLR4 (clone HTA125)	Biolegend	312811	1:50
anti-CD206 (clone 15-2)	Biolegend	321140	1:50
anti-CD163 (clone GHI/61)	Biolegend	333630	1:100
anti-TNF (clone MAb11)	Biolegend	502948	1:40
anti-IL-6 (clone MQ2-13A5)	Biolegend	501107	1:40
Antibodies (myeloid cell panel, Syngeneic MB49 urothelial cancer model)			
CD45 (clone 30-F11)	Biolegend	103128	1:100
CD124 (IL-4Ra) (clone I015F8)	Biolegend	144804	1:50
I-a/I-e (clone M5/114.15.2)	Biolegend	107645	1:100
F4/80 (clone BM8)	Biolegend	123147	1:100
CD206 (clone C068C2)	Biolegend	141721	1:200
TNF (clone MP6-XT22)	Biolegend	506345	1:40
IL-10 (clone JES5-16E3)	Thermo Fisher	505022	1:50
Antibodies (lymphoid cell panel, Syngeneic MB49 urothelial cancer model)			
CD45 (clone 30-F11)	Biolegend	103128	1:200
CD25 (clone PC61)	Biolegend	102033	1:100
CD3 (clone 17A2)	Biolegend	100248	1:50
CD4 (clone GK1.5)	Biolegend	100434	1:100
CD8a (clone 53-6.7)	Biolegend	100741	1:100
FOXP3 (clone MF-14)	Biolegend	126406	1:50
Mouse IFN-γ (clone XMG1.2)	Biolegend	505835	1:50

CD69 (clone H1.2F3)	Biolegend	104536	1:100
CD38 (clone 90)	Biolegend	102712	1:100
Reagents/Kits			
Name	**Source**	**#Cat.**	
Protein transport inhibitor cocktail	eBioscience	00-4980-03	
Zombie Aqua™ Fixable Viability Kit	Biolegend	423101	
TruStain FcX™	Biolegend	101320	
Fixation and Permeabilization Buffer Set	Biolegend	421403	
Human TruStain FcX™	Biolegend	422302	
True-Stain Monocyte Blocker™	Biolegend	426102	
2-NBDG Glucose Uptake Assay Kit	Abcam	ab235976	
ELISA			
Mouse ELISA Kits			
TNF- DuoSet	R and D Systems	DY410	
IL-6 DuoSet	R and D Systems	DY406	
IFN- DuoSet	R and D Systems	DY485	
CCL2/JE/MCP-1 DuoSet	R and D Systems	DY479	
LEGEND MAX™ Mouse IFN-β	Biolegend	439407	
Human ELISA Kits			
TNF- DuoSet	R and D Systems	DY210	
IL-6 DuoSet	R and D Systems	DY206	
IFN-β ELISA Kit	PBL Assay Science	41410-2	
Rat ELISA Kits			
IFN- Quantikine	R and D Systems	RIF00	
TNF- Quantikine	R and D Systems	RTA00	

IL-2 Quantikine	R and D Systems	R2000
Chromatin Immunoprecipitation		
ChIP Antibodies		
Histone H3K9me3 (H3K9 Trimethyl) Polyclonal Antibody	epigentek	A-4036-100
Anti-Histone H3 (tri methyl K4) antibody - ChIP Grade	abcam	ab8580
ChIP Reagents		
BSA	Sigma-Aldrich	A3294
Salmon Sperm DNA	Thermo Fisher Scientific	15632011,
HEPES	Sigma-Aldrich	H3375
Formaldehyde	Sigma-Aldrich	252549
EGTA	Sigma-Aldrich	03777
EDTA	Sigma-Aldrich	E6758
TritonX-100	Sigma-Aldrich)	T8787
SDS	Sigma-Aldrich	71736
NaHCO3	Sigma-Aldrich	5761
Nuclease free water	Thermo Fisher Scientific	AM9930
SYBR green dye	Applied Biosystems	4385614

Supplementary Table S2: Cloning and PCR primers used in the study

Cloning primers used in the study		
Accession Number	**Gene**	**Sequence (5'-3')**
	pSD5hsp60.MT3692 (F)	GGGCATCATATGCACGCTGTGACTCGTC
	pSD5hsp60.MT3692 (R)	GGGACGCGTTATTGATCGCTGATGGTCGATT
	Kanamycin cassette (F)	GAGAAAACTCACCGAGGCAG
	Kanamycin cassette (R)	GTATTTCGTCTCGCTCAGGC
32287254	*M.tb* sigH (F)	GCGATGGTGGCTTCTCCCTCG
	M.tb sigH (R)	CCATCTTGCACAGCTCGCGTAG
qPCR primers used in the study		
Mouse Primers		
11461	Mouse.β actin (F)	TAAGGCCAACCGTGAAAAGATG
	Mouse.β actin (R)	CTGGATGGCTACGTACATGGCT
21926	Mouse.TNF-α (F)	GACCCTCACACTCAGATCATC
	Mouse.TNF-α (R)	GCTGCTCCTCCACTTGGT
15977	Mouse.IFN-β (F)	CCACAGCCCTCTCCATCAAC
	Mouse.IFN-β (R)	CTCCGTCATCTCCATAGGGA
16193	Mouse.IL6 (F)	CTGCAAGAGACTTCCATCCAG
	Mouse.IL6 (R)	CAGGTCTGTTGGGAGTGG
15978	Mouse.IFN (F)	AGCGGCTGACTGAACTCAGATTGT
	Mouse.IFN (R)	GTCACAGTTTTCAGCTGTATAGGG
16176	Mouse.IL1 (F)	GGAGAGTGTGGATCCCAA
	Mouse.IL1 (R)	GTGGAGTTTGAGTCTGCAG
20296	Mouse.MCP1 (F)	GGCTCAGCCAGATGCAGTTAAC
	Mouse.MCP1 (R)	GATCCTCTTGTAGCTCTCCAGC
16160	Mouse.IL12b (F)	GAAAGACGTTTATGTTGTAGAGG
	Mouse.IL12b (R)	GACTCCATGTCTCTGGTCTG
17329	Mouse.CXCL9 (F)	GGAGTTCGAGGAACCCTAGTG

	Mouse.CXCL9 (R)	GGGATTTGTAGTGGATCGTGC
15945	Mouse.CXCL10 (F)	GTGGGACTCAAGGGATCCCTCTC
	Mouse.CXCL10 (R)	GCTTCCCTATGGCCCTCATTC
18126	Mouse.NOS2 (F)	GTTCTCAGCCCAACAATACAAG
	Mouse.NOS2 (R)	GGAACATTCTGTGCTGTCCC
20299	Mouse.CCL22 (F)	CTCTGATGCAGGTCCCTATGGTG
	Mouse.CCL22 (R)	GGCAGAGGGTGACGGATGTAG
Human Primers		
26827	Human. RNU6A (F)	CTCGCTTCGGCAGCACATATAC
	Human. RNU6A (R)	AATATGGAACGCTTCACGAATTTG
3456	Human.IFNβ (F)	CAACTTGCTTGGATTCCTACAAAG
	Human.IFNβ (R)	TATTCAAGCCTCCCATTCAATTG
3569	Human.IL6 (F)	GGTACATCCTCGACGGCATCT
	Human.IL6 (R)	GTGCCTCTTTGCTGCTTTCAC
Rat Primers		
64367	Rat.PPIB (F)	CAGGATTCATGTGCCAGGGT
	Rat.PPIB (R)	CCAAAGACCACATGCTTGCC
24481	Rat.IFN-β (F)	GAGTCTTCACACTCCTGGC
	Rat.IFN-β (R)	GTCCTTCAGGCATGAGACAG
298210	Rat.IFN–α (F)	GCGTTCCTGCTGTGCTTCTC
	Rat.IFN-α (R)	CCATTCAGCTGCCTCAGGAGC
25712	Rat.IFN–γ (F)	CGTCTTGGTTTTGCAGCTCT
	Rat.IFN-γ (R)	CGTCCTTTTGCCAGTTCCTC
24599	Rat. iNOS (F)	GGTGAGGGGACTGGACTTTTAG
	Rat. iNOS (R)	TTGTTGGGCTGGGAATAGCA
245920	Rat.IP10 (F)	TCCACCTCCCTTTACCCAGT
	Rat.IP10 (R)	AGAGCTAGGAGAGCCGTCAT
24770	Rat.MCP-1 (F)	CAGGTCTCTGTCACGCTTCTG
	Rat.MCP-1 (R)	GCCAGTGAATGAGTAGCAGCAG
25542	Rat.MIP-1α (F)	ACAAGCGCACCCTCTGTTAC
	Rat.MIP-1α (R)	GGTCAGGAAAATGACACCCG
24494	Rat.IL-1β (F)	GACTTCACCATGGAACCCGT

	Rat.IL-1β (R)	GGAGACTGCCCATTCTCGAC
24835	Rat.TNF-α (F)	CGTCCCTCTCATACACTGG
	Rat.TNF-α (R)	CATGCTTTCCGTGCTCATG
59086	Rat.TGF-β (F)	TGACGTCACTGGAGTTGTCC
	Rat.TGF-β (R)	CCTCGACGTTTGGGACTGAT
25325	Rat.IL-10 (F)	CCTCTGGATACAGCTGCGAC
	Rat.IL-10 (R)	TGCCGGGTGGTTCAATTTTTC
ChIP-PCR Primers		
	Human.GAPDH (F)	TACTAGCGGTTTTACGGGCG
	Human.GAPDH (R)	TCGAACAGGAGGAGCAGAGAGCGA
	Human.IL-6 (F)	CGGTGAAGAATGGATGACCT
	Human.IL-6 (R)	AAACGAGACCCTTGCACAAC
	Human.TNF-α (F)	ATCAGTCAGTGGCCCAGAAGACCC
	Human.TNF-α (R)	CCACGTCCCGGATCATGCTTCAG

Source Data

Improved bladder cancer antitumor efficacy with a recombinant BCG that releases a STING agonist

Figure 2b (i)

MNU Rat Bladder (Post BCG Immunotherapy) qPCR
Fold Expression (Log2)
IFN-β gene

	Ifnb			
	Control	Untreated	BCG-WT (Tice)	BCG-*disA* -OE (Tice)
Animal 1	0.9462	0.4323	0.3983	3.3258
Animal 2	0.7949	0.8570	0.3026	4.0350
Animal 3	1.4769	0.8532	0.3885	6.7943
Animal 4	1.6185	0.8145	0.3947	2.4513
Animal 5	0.7193	0.4325	0.4030	2.4153

MNU Rat Bladder (Post BCG Immunotherapy) qPCR
Fold Expression (Log2)
IFN-γ gene

	Ifng			
	Control	Untreated	BCG-WT (Tice)	BCG-*disA* -OE (Tice)
Animal 1	1.3668	0.1644	0.5392	3.6505
Animal 2	0.7741	0.1330	0.6280	4.7526
Animal 3	1.5244	0.2770	0.4786	2.6071
Animal 4	0.9933	0.1577	0.5626	2.5401
Animal 5	0.9765	0.2184	0.6620	2.0162

MNU Rat Bladder (Post BCG Immunotherapy) qPCR
Fold Expression (Log2)
TNF-α gene

	Tnfa			
	Control	Untreated	BCG-WT (Tice)	BCG-*disA* -OE (Tice)
Animal 1	1.0537	1.1987	2.2263	5.0408
Animal 2	0.8277	1.5919	4.9580	5.0596
Animal 3	1.1050	2.7742	4.7815	5.1397
Animal 4	1.1006	2.8183	2.2567	4.6265
Animal 5	0.9130	2.5765	4.9526	4.7647

Figure 2b (ii)

MNU Rat Bladder (Post BCG Immunotherapy) qPCR
Fold Expression (Log2)
IL-1β gene

	Il1b			
	Control	Untreated	BCG-WT (Tice)	BCG-*disA* -OE (Tice)
Animal 1	1.6453	1.3032	4.0929	3.8334
Animal 2	1.4692	1.0493	1.5417	5.7733
Animal 3	0.2676	2.3949	2.4456	5.4485
Animal 4	1.3872	3.6081	1.8949	5.9633
Animal 5	0.2308	3.6083	1.8901	5.9916

MNU Rat Bladder (Post BCG Immunotherapy) qPCR
Fold Expression (Log2)
CXCL10 gene

	Cxcl10			
	Control	Untreated	BCG-WT (Tice)	BCG-*disA* -OE (Tice)
Animal 1	1.3507	0.1813	0.2843	2.4623
Animal 2	0.8683	0.1763	0.2710	2.7094
Animal 3	0.9417	0.1734	0.5572	2.3360
Animal 4	0.8394	0.2330	0.3326	4.4101
Animal 5	1.1473	0.3051	0.2727	2.9344

MNU Rat Bladder (Post BCG Immunotherapy) qPCR
Fold Expression (Log2)
MCP-1 gene

	Mcp1			
	Control	Untreated	BCG-WT (Tice)	BCG-*disA* -OE (Tice)
Animal 1	1.2807	0.4347	0.3453	2.8489
Animal 2	1.0746	0.5138	0.4674	3.1102
Animal 3	1.0435	0.507	0.3142	4.7347
Animal 4	0.8860	0.6558	0.2760	4.4665
Animal 5	0.7153	0.6598	0.2898	2.1945

Figure 2b (iii)

MNU Rat Bladder (Post BCG Immunotherapy) qPCR
Fold Expression (Log2)
MIP-1α gene

	Mip1a			
	Control	Untreated	BCG-WT (Tice)	BCG-*disA* -OE (Tice)
Animal 1	1.1379	0.1872	0.3376	2.1696
Animal 2	0.8621	0.1066	0.3569	1.8937
Animal 3	0	0.1557	0.3246	1.0737
Animal 4	0.8267	0.1587	0.2431	1.8990
Animal 5	1.0137	0.1222	0.3550	1.2796

MNU Rat Bladder (Post BCG Immunotherapy) qPCR
Fold Expression (Log2)
IL-10 gene

	Il10			
	Control	Untreated	BCG-WT (Tice)	BCG-*disA* -OE (Tice)
Animal 1	1.4684	6.1882	4.7483	2.0002
Animal 2	0.6358	7.2067	4.1929	2.9396
Animal 3	1.6621	6.8448	1.7800	2.5655
Animal 4	0.6174	6.3872	3.0441	3.8789
Animal 5	0.6163	6.2583	3.0442	3.8785

MNU Rat Bladder (Post BCG Immunotherapy) qPCR
Fold Expression (Log2)
TGF-β gene

	Tgfb			
	Control	Untreated	BCG-WT (Tice)	BCG-*disA* -OE (Tice)
Animal 1	1.0998	10.7662	2.2188	2.1424
Animal 2	0.8343	6.5788	3.2697	2.2181
Animal 3	1.1785	7.2088	2.7960	5.5651
Animal 4	0.9414	6.7679	2.4813	2.5642
Animal 5	0.9459	6.3653	2.4116	2.5671

Figure 2b (iv)

MNU Rat Bladder (Post BCG Immunotherapy) qPCR
Fold Expression (Log2)
Nos2 gene

	Nos2			
	Control	Untreated	BCG-WT (Tice)	BCG-*disA* -OE (Tice)
Animal 1	1.1946	4.9202	8.9481	49.8755
Animal 2	0.1469	3.9075	7.8584	34.1369
Animal 3	0.7264	5.7335	8.9911	48.7897
Animal 4	1.4347	3.6855	5.9194	56.3878
Animal 5	1.4974		5.7084	56.1033

Figure 2d

Tumor Involvement Index (MNU Rat Bladder Post BCG Immunotherapy)

	Untreated	BCG-WT (Tice)	BCG-*disA* -OE (Tice)
Animal 1	600	0	0
Animal 2	2500	2700	200
Animal 3	200	0	400
Animal 4	200	0	200
Animal 5	500	300	0
Animal 6	300	1500	0
Animal 7	3500	100	0
Animal 8		0	300
Animal 9		500	400
Animal 10		400	0
Animal 11		0	0

Tumor staging was performed by 2 board-certified genitourinary pathologists (A.S.B., A.M.) blinded to treatment groups. Specimens were classified based on the percentage of involvement of abnormal tissue.

Figure 2e

Histopathology
(MNU Rat Model of NMIBC)

Animal	Pathologic Stage
CTRL 1	HGT2
CTRL 2	CIS
CTRL 4	CIS
CTRL 5	CIS
CTRL 6	CIS
BCG WT 1	dysplasia
BCG WT 2	HGT1
BCG WT 3	dysplasia
BCG WT 4	CIS
BCG WT 5	dysplasia
BCG OE 1	dysplasia
BCG OE 2	dysplasia
BCG OE 3	CIS
BCG OE 4	CIS
BCG OE 5	dysplasia

Animal	Pathologic Stage
Control 1	LGTa
Control 2	HGT2
Control 3	LGTa, squamous metaplasia
Control 4	HGT1
Control 5	CIS
Control 6	CIS
WT TICE 1	HGT1
WT TICE 2	CIS
WT TICE 3	CIS
WT TICE 4	CIS
WT TICE 5	CIS
WT TICE 6	dysplasia
OE TICE 1	LGTa
OE TICE 2	dysplasia
OE TICE 3	CIS
OE TICE 4	LGTa
OE TICE 5	dysplasia
WT Pasteur1	HGT1 (90%) squamous differentiation
WT Pasteur2	CIS
WT Pasteur3	dysplasia
WT Pasteur4	LGTa
WT Pasteur5	CIS
OE Pasteur 1	dysplasia
OE Pasteur 2	LGTa
OE Pasteur 3	CIS
OE Pasteur 4	dysplasia
OE Pasteur 5	dysplasia

OE = BCG-*disA* -OE

Staging was performed by a blinded by a board-certified pathologist
dysplasia= abnormal appearing urothelium falling short of criteria for carcinoma in situ
CIS= carcinoma in situ
LGTa= low grade non invasive
HGTa = high grade non invasive
HGT1 = high grade invasive into the lamina propria
HGT2 = high grade invasive into the muscle

Figure 2g

Ki67 Staining (IHC) (MNU Rat Bladder Post BCG Immunotherapy)

	Untreated	BCG-WT (Tice)	BCG-*disA* -OE (Tice)
Animal 1	15	20	10
Animal 2	40	20	15
Animal 2	15	10	20
Animal 4	40	10	5
Animal 5	15	20	5
Animal 6	20	30	10
Animal 7	30	10	5
Animal 8	20	10	20
Animal 9	30	20	15
Animal 10	20	20	2
Animal 11	15	10	5
Animal 12	30	10	5
Animal 13	10	20	20
Animal 14	30	10	15
Animal 15	20	30	10
Animal 16	10	10	10
Animal 17		10	10
Animal 18		20	20
Animal 19		10	15
Animal 20		30	10
Animal 21		10	

All slides were scored blinded by board certified pathologist
Ki67 IHC Scores represent % of positive cells in urothelium

Figure 2h

CD68 IHC Score (MNU Rat Bladder Post BCG Immunotherapy)

	Untreated	BCG-WT (Tice)	BCG-*disA* -OE (Tice)
Animal 1	2	1	3
Animal 2	1	3	2
Animal 3	1	1	2
Animal 4	2	3	2
Animal 5	2	1	2

CD86 IHC Score (MNU Rat Bladder Post BCG Immunotherapy)

	Untreated	BCG-WT (Tice)	BCG-*disA* -OE (Tice)
Animal 1	0	0	1
Animal 2	0	0	0
Animal 3	1	0	0
Animal 4	0	1	1
Animal 5	1	0	1

CD206 IHC Score (MNU Rat Bladder Post BCG Immunotherapy)

	Untreated	BCG-WT (Tice)	BCG-*disA* -OE (Tice)
Animal 1	2	0	0
Animal 2	1	1	0
Animal 3	1	1	1
Animal 4	1	1	0
Animal 5	1	0	0

All slides were scored blinded by board certified pathologist
CD68, CD206, CD86 IHC SCORES
1= Positive isolated cells
2= Clusters of up to 10 positive cells
3= Greater than 10 positive cells/cluster

Figure 3b

Tumor Volume (mm3) (Mouse MB49 Tumors, C57BL/6 Female Mice)
Syngeneic MB49 Model of Urothelial Cancer

	Vehicle	Vehicle	Vehicle	Vehicle	Vehicle	Vehicle	Vehicle	Vehicle
	Animal 1	Animal 2	Animal 3	Animal 4	Animal 5	Animal 6	Animal 7	Animal 8
D1	0	0	0	0	0	0	0	0
D10	87.99	78.96	28.42	57.14	47.07	47.01	40.95	60.00
D14	425.38	201.34	379.94	322.70	165.39	250.57	212.55	216.12
D18	669.83	221.31	660.34	495.39	165.58	514.45	496.02	248.55
D22	1041.45	316.99	783.46	463.34	250.82	643.67	446.31	210.12

	BCG-WT (Pasteur)	BCG-WT (Pasteur)	BCG-WT (Pasteur)	BCG-WT (Pasteur)	BCG-WT (Pasteur)	BCG-WT (Pasteur)	BCG-WT (Pasteur)	BCG-WT (Pasteur)
	Animal 1	Animal 2	Animal 3	Animal 4	Animal 5	Animal 6	Animal 7	Animal 8
D1	0	0	0	0	0	0	0	0
D10	71.30	69.26	58.60	56.14	48.06	46.52	33.95	21.08
D14	155.32	158.67	140.94	168.40	180.66	166.57	160.94	136.87
D18	213.56	237.50	238.94	365.81	97.51	212.90	196.10	105.52
D22	252.24	280.65	251.85	444.25	32.76	221.53	213.04	181.35

	BCG-*disA* -OE (Pasteur)	BCG-*disA* -OE (Pasteur)	BCG-*disA* -OE (Pasteur)	BCG-*disA* -OE (Pasteur)	BCG-*disA* -OE (Pasteur)	BCG-*disA* -OE (Pasteur)	BCG-*disA* -OE (Pasteur)	BCG-*disA* -OE (Pasteur)
	Animal 1	Animal 2	Animal 3	Animal 4	Animal 5	Animal 6	Animal 7	Animal 8
D1	0	0	0	0	0	0	0	0
D10	102.81	74.22	32.79	54.46	48.86	45.89	38.24	58.00
D14	79.38	109.66	110.68	43.96	104.04	122.23	200.26	63.15
D18	135.72	174.26	193.18	41.82	168.83	150.17	93.63	83.34
D22	72.14	156.35	174.09	56.27	194.91	109.07	151.79	198.25

Figure 3c

% CD3+ of CD45 cells (MB49 Tumors)
Syngeneic MB49 heterotopic tumor model)
Flow Cytometry Analyses

Animal	C57BL/6 WT + Saline	STING$^{-/-}$ (C57BL/6J-Tmem173gt/J) + Saline	C57BL/6 WT + BCG-WT (Tice)	STING$^{-/-}$ (C57BL/6J-Tmem173gt/J) + BCG-WT (Tice)	C57BL/6 WT + BCG-*disA* -OE (Tice)	STING$^{-/-}$ (C57BL/6J-Tmem173gt/J) + BCG-*disA* -OE (Tice)
A1	13.7	6.9	42.2	16.0	42.7	64.1
A2	11.3	7.1	21.2	16.5	36.4	16.2
A3	19.5	6.3	25.0	13.5	73.6	6.4
A4	14.2	8.9	28.9	19.8	34.4	14.3
A5	13.6	6.8	30.6	15.8	70.5	36.0
A6	14.1	8.0	35.0	21.1	23.9	16.8

A: Animal

Figure 3d

% CD25+CD69+ of CD8 T cells (MB49 Tumors)
Syngeneic MB49 heterotopic tumor model)
Flow Cytometry Analyses

Animal	C57BL/6 WT + Saline	STING$^{-/-}$ (C57BL/6J-Tmem173gt/J) + Saline	C57BL/6 WT + BCG-WT (Tice)	STING$^{-/-}$ (C57BL/6J-Tmem173gt/J) + BCG-WT (Tice)	C57BL/6 WT + BCG-*disA* -OE (Tice)	STING$^{-/-}$ (C57BL/6J-Tmem173gt/J) + BCG-*disA* -OE (Tice)
A1	1.88	1.76	12.9	2.54	30.5	7.82
A2	0.97	0.38	0.58	18.5	25.4	4.17
A3	9.20	0.64	9.75	0.28	26.6	0
A4	1.60	0.80	6.48	9.50	23.7	4.58
A5	2.13	1.14	8.61	2.36	27.3	22.8
A6	1.09	0.21	13.6	17.3	19.1	19.3

A: Animal

Figure 3e

% TNF-α+ of F4/80+CD11b+ cells (MB49 Tumors)
Syngeneic MB49 heterotopic tumor model)
Flow Cytometry Analyses

Animal	C57BL/6 WT + Saline	STING$^{-/-}$ (C57BL/6J-Tmem173gt/J) + Saline	C57BL/6 WT + BCG-WT (Tice)	STING$^{-/-}$ (C57BL/6J-Tmem173gt/J) + BCG-WT (Tice)	C57BL/6 WT + BCG-*disA* -OE (Tice)	STING$^{-/-}$ (C57BL/6J-Tmem173gt/J) + BCG-*disA* -OE (Tice)
A1	11.6	5.9	29.1	19.6	36.2	12.6
A2	7.1	3.8	18.8	28.1	39.2	17.9
A3	10.3	5.1	28.6	12.5	33.8	9.81
A4	12.3	4.6	26.1	24.4	38.0	15.6
A5	10.4	3.0	28.2	16.8	34.1	13.7
A6	10.3	7.8	23.6	35.9	41.0	17.3

A: Animal

Figure 4b

Lung Bacillary Burden in BALB/c Mice after BCG Infection
D1 Implantation: raw CFU per lung and log10 CFU per lung

Half of total lung homogenate plated on each of 2 plates

CFU counts per plate (each animal lung plated in duplicate) (D1 implantation)				
Strain	**Plate 1**	**Plate 2**	**CFU (total)**	**Log10cfu**
BCG-WT (Tice)				
A1	209	195	404	2.607
A2	109	172	281	2.450
A3	110	352	462	2.666
BCG-*disA* -OE (Tice)				
A1	378	73	451	2.655
A2	376	66	462	2.666
A3	214	110	324	2.512

Lung Bacillary Burden in BALB/c Mice after BCG.
Infection D28 (log10 CFU per lung)

	BCG-WT (Tice)	**BCG-*disA* -OE (Tice)**
Animal 1	6.243	5.933
Animal 2	6.347	5.861
Animal 3	6.294	5.834
Animal 4	6.142	5.774
Animal 5	6.251	5.704

Figure 4d

Lung Bacillary Burden in SCID Mice after BCG Infection D1 Implantation (log10 CFU per lung)

	BCG-WT (Tice)	BCG-*disA* -OE (Tice)
Animal 1	1.152	1.179
Animal 2	1.170	1.185

Figure 4e (i)

Time to Death (SCID Mice after BCG Infection)

Days after Infection	BCG-WT (Tice)	BCG-*disA* -OE (Tice)	No treatment
60			
61			
62			
63			
64			
65			
66			
67			
68			
69			
70			
71			
72			
73	1		
74			
75			
76			
77			
78	1		
79			
80			
81			
82			
82	1		
83			
84			
85			
86	1		
87			
88			
89			
90			
91			
92			
92			
93			

Figure 4e (ii)

94			
95			
96			
97			
98			
98			
99			
100			
101			
102			
103			
104			
105			
106			
107			
108			
109		1	
110			
111			
112			
113			
114			
115			
116			
117			
118			
119			
120			
121		1	
122			
123			
124			
125			
126			
127			
128		1	
128	1		
128			
128			
129			
130			

Figure 4e (iii)

131		1	
132	1		
133		1	
133	1		
133			
134			
134	1		
135			
136		1	
136	1		
136			
136			
137			
138	1		
139			
140			
141			
142			
143			
144			
145			
146			
147			
148			
149			
150			
151			
152			
153			
154			
155		1	
156			
157			
158			
159			
159			
160			
161			
162			
163			
164			

Figure 4e (iv)

165			
166			
167		1	
168			0
169			0
170			0
171		1	0
172			0
173			0
174			0
175			0
176			0
177		1	0

Figure 5a

Raw Lucia ISG Reporter Assay (IRF Induction; RLU)

	R1	R2	R3	R4
No treatment	13110	11060	11560	12020
BCG-WT (Tice)	141140	130610	169150	174280
BCG-disA-OE (Tice)	298050	293190	288970	333100
LPS (E.coli)	352020	349970	349410	330760
c-di-AMP (50 μg/ml)	257170	257280	267580	273880

Figure 5b

IFN-β (BMDM) (ELISA)
Concentration in pg/ml

	WT-1	WT-2	WT-3	STING KO-1	STING KO-2	STING KO-3
No treatment	10.0	8.5	9.0	5.0	4.8	6.1
BCG-WT (Tice)	19.9	22	18.9	12.3	15.6	16.8
BCG-*disA* -OE (Tice)	45.0	48.0	42.0	13.2	14.9	11.2
c-di-AMP (50 μg/ml)	60.7	61.9	59.9	7.3	6.8	7.9

WT: BMDM C57BL/6 (F)

STING KO: BMDM "STING-/- (C57BL/6J-Tmem173gt/J)

Figure 5c

ELISA (Bone Marrow-Derived Macrophages)
IFN-β (ELISA) (pg/ml)

	NT-1	NT-2	NT-3	WT-1	WT-2	WT-3	OE-1	OE-2	OE-3	LPS-1	LPS-2	LPS-3
J774.1	4.79	5.68	5.56	13.99	10.29	10.76	19.75	20.75	25.83	31.70	15.81	16.79
HMDM	3.57	6.00	5.89	13.66	15.18	11.86	38.50	41.37	35.89	57.65	62.96	56.58

NT: No treatment
WT: BCG-WT (Tice)
OE: BCG-disA-OE (Tice)
LPS: LPS (E.coli)

Figure 6a

Macrophage reprogramming (BMDM infection with BCG) (Flow cytomeric analyses)
MOI (20:1)

	NT-1	NT-2	NT-3	NT-4	WT (P)-1	WT (P)-2	WT (P)-3	WT (P)-4	OE (P)-1	OE (P)-2	OE (P)-3	OE (P)-4
%TNFα+ MHCII+ of CD11b+ F4/80+	0.58	0.75	0.60	0.76	16.0	16.1	22.4	23.3	25.6	23.5	21.6	22.3

NT: No treatment
WT (P): BCG-WT (Pasteur)
OE (P): BCG-disA-OE

Figure 6b

Macrophage reprogramming (BMDM infection with BCG) (Flow cytomeric analyses) MOI (20:1)

	NT-1	NT-2	NT-3	NT-4	WT (P)-1	WT (P)-2	WT (P)-3	WT (P)-4	OE (P)-1	OE (P)-2	OE (P)-3	OE (P)-4
%CD206+ CD124+ of CD11b+ F4/80+	79.7	81.8	80.5	79.5	43.6	41.1	37.5	36.4	20.0	19.3	17.8	17.2

NT: No treatment
WT (P): BCG-WT (Pasteur)

Figure 6c

Macrophage reprogramming (BMDM infection with BCG) (Flow cytomeric analyses) MOI (20:1)

	NT-1	NT-2	NT-3	NT-4	WT (P)-1	WT (P)-2	WT (P)-3	WT (P)-4	OE (P)-1	OE (P)-2	OE (P)-3	OE (P)-4
% IL-10 of CD206 +CD124+	3.23	3.36	3.21	3.34	22.3	17.7	31.7	29.8	7.31	4.32	9.46	6.02

NT: No treatment
WT (P): BCG-WT (Pasteur)

Figure 6d

MDSC population in mouse BMDM after BCG infection (Flow cytomeric analyses)
MOI (20:1)

	NT-1	NT-2	NT-3	NT-4	WT(P)-1	WT(P)-2	WT(P)-3	WT(P)-4	OE(P)-1	OE(P)-2	OE(P)-3	OE(P)-4
%M-MDSC of $CD45^+$	0	0	0	0	1.78	2.21	1.59	2.26	0.55	0.49	0	0

NT: No treatment
WT (P): BCG-WT (Pasteur)
OE (P): BCG-disA-OE (Pasteur)

Figure 6e

MDSC population in mouse BMDM after BCG infection (Flow cytomeric analyses)
MOI (20:1)

	NT-1	NT-2	NT-3	NT-4	WT(P)-1	WT(P)-2	WT(P)-3	WT(P)-4	OE(P)-1	OE(P)-2	OE(P)-3	OE(P)-4
% IL-10 of M-MDSC	0	0	0	0	18.5	30.7	18.3	22.0	0	2.28	0	0

NT: No treatment
WT (P): BCG-WT (Pasteur)
OE (P): BCG-disA-OE

Figure 6f

In Vitro Phagocytic Activity
Bone Marrow-Derived Macrophages (BMDM)
Mean Fluorescence Intensity

NT-1	NT-2	NT-3	WT-1	WT-2	WT-3	OE-1	OE-2	OE-3
782	734	754	1363	1407	2129	6271	5497	2605

NT: No treatment
WT: BCG-WT (Tice)
OE: BCG-disA-OE (Tice)

Figure 6h

Autophagic Flux (LC3B Staining)
Bone Marrow-Derived Macrophages (BMDM)

NT-1	NT-2	NT-3	WT-1	WT-2	WT-3	OE-1	OE-2	OE-3
0.19	0.20	0.12	2.50	2.40	1.90	3.16	2.85	2.45

Autophagic Targeting (LC3B-BCG colocalization)
Bone Marrow-Derived Macrophages (BMDM)

WT-1	WT-2	WT-3	OE-1	OE-2	OE-3
27.8	25.0	30.6	42.5	40.0	39.2

NT: No treatment

WT: BCG-WT (Tice)

OE: BCG-disA-OE (Tice)

Figure 6j

Autophagic Targeting (p62-BCG colocalization)
Bone Marrow-Derived Macrophages (BMDM)

Group	Nuclei	BCG bacilli	Colocalized BCG bacilli with p62	% Colocalization
WT-1	4	12	3	25.0
WT-1	4	8	2	25.0
WT-1	4	12	2	16.6
OE-1	4	14	7	50.0
OE-2	4	14	6	42.9
OE-3	4	12	4	33.3

Figure 7a

TNF-α qPCR (Human Monocytes from Healthy Donors)
Fold-change in Expression

	WT	OE
D1	7.1	17.5
D2	6.8	17.7
D3	5.2	16.4
D4	10.0	15.4
D5	9.8	13.7
D6	10.8	14.9

WT: BCG-WT (Tice)

OE: BCG-disA-OE (Tice)

IL-6 qPCR (Human Monocytes from Healthy Donors)
Fold-change in Expression

	WT	OE
D1	1237	4169
D2	793	2806
D3	730	3168
D4	765	1562
D5	633	1457
D6	1037	2083

WT: BCG-WT (Tice)

OE: BCG-disA-OE (Tice)

Figure 7c

Chromatin Immunoprecipitation-Polymerase Chain Reaction (ChIP-PCR)
(Human Monocytes)
Chromatin Activation Mark (H3K4Me3) after BCG Training
Human Monocytes
IL-6 Promoter (% Input)

	NT-1	NT-2	NT-3	NT-1 +PAM3CK4	NT-2 +PAM3CK4	NT-3 +PAM3CK4
Donor	0.024	0.054	0.14	0.63	0.12	0.22

	WT-1 +RPMI	WT-2 +RPMI		WT-1 + PAM3CSK4	WT-2 + PAM3CSK4	WT-3 + PAM3CSK4
Donor	0.69	1.12		6.56	6.87	7.26

	OE-1 +RPMI	OE-2 +RPMI	OE-3 +RPMI	OE-1 +PAM3CSK4	OE-2 +PAM3CSK4	OE-3 +PAM3CSK4
Donor	2.29	1.78	2.32	19.90	19.60	17.10

Figure 7d

In Vitro BCG Training
IL-6 ELISA (pg/ml) (Human Monocytes after BCG Training and Stimulation)

NT-1	NT-2	NT-3	Rest-1	Rest-2	Rest-3	Rest-1 + PAM3CSK 4 (Stim.)	Rest-2 + PAM3CSK 4 (Stim.)	Rest-3 + PAM3CS K4 (Stim.)
15.6	12.7	19	13.7	14.2	14.3	408	372	396

WT-1 + Rest	WT-2 +Rest	WT-3 +Rest	WT-1 +Rest +PAM3CS K4 (Stim.)	WT-2 +Rest +PAM3CS K4 (Stim.)	WT-3 +Rest +PAM3CS K4 (Stim.)
268	226	231	431	445	449

OE-1 +Rest	OE-2 +Rest	OE-3 +Rest	OE-1 +Rest +PAM3CS K4 (Stim.)	OE-2 +Rest +PAM3CS K4 (Stim.)	OE-3 +Rest +PAM3CS K4 (Stim.)
313	388	376	555	565	541

NT: No treatment
WT: BCG-WT (Tice)
OE: BCG-disA-OE (Tice)
Stim.: Stimulation

Figure 7e

In Vitro BCG Training
TNF-α ELISA (pg/ml) (Human Monocytes after BCG Training and Stimulation)

NT-1	NT-2	NT-3	Rest-1	Rest-2	Rest-3	Rest-1+ PAM3CSK4 (Stim.)	Rest-2+ PAM3CSK4 (Stim.)	Rest-3+ PAM3CSK4 (Stim.)
49.9	55.5	76.4	9.0	39.5	42.4	1251	1238	1322

WT-1 +Rest	WT-2 +Rest	WT-3 +Rest	WT-1 +Rest +PAM3CSK4 (Stim.)	WT-2 +Rest +PAM3CSK4 (Stim.)	WT-3 +Rest +PAM3CSK4 (Stim.)
254	292	273	1736	1793	1760

OE-1 +Rest	OE-2 +Rest	OE-3 +Rest	OE-1 +Rest +PAM3CSK4 (Stim.)	OE-2 +Rest +PAM3CSK4 (Stim.)	OE-3 +Rest +PAM3CSK4 (Stim.)
371	378	379	2000	2266	2381

NT: No treatment
WT: BCG-WT (Tice)
OE: BCG-disA-OE (Tice)
Stim.: Stimulation

Figure 8a

Relative Abundance of Intracellular Metabolite (HMDM)

	WT-1	WT-2	OE-1	OE-2
Glucose	68002	61340	103234	102895
Lactate	45899539	30163300	81380397	87077835
Tryptophan	1159366	1636769	1945251	1898404
Kynurenine	649069	745098	41300	40942

WT: BCG-WT (Tice)

OE: BCG-disA-OE (Tice)

Figure 8b

Relative Abundance of Intracellular Metabolite (BMDM)

	WT-1	WT-2	WT-3	WT-4	OE-1	OE-2	OE-3	OE-4
Glucose	144972	94300	35240	112712	223466	223982	155474	154959
Lactate	309000000	367000000	420000000	408000000	546000000	539000000	537000000	535000000
Tryptophan	5095958	6000815	3667625	6288585	23414256	11263863	10891419	7355621

	HK-WT-1	HK-WT-2	HK-WT-3	HK-WT-4	HK-OE-1	HK-OE-2	HK-OE-3	HK-OE-4
Glucose	21397	83754	51961	97683	58805	128042	83549	91445
Lactate	366000000	352000000	295000000	210000000	265000000	359000000	314000000	319000000
Tryptophan	4930796	5327760	6979848	10649448	4408661	3109284	3977229	6137930

WT: BCG-WT (Tice)
OE: BCG-disA-OE (Tice)
HK-WT: Heat-Killed BCG-WT (Tice)
HK-OE: Heat-Killed BCG-disA-OE (Tice)

Figure S1a

***disA*-qPCR in log-phase BCG cultures of BCG-WT (Tice and BCG-*disA*-**

	WT-1	WT-2	WT-3	OE-1	OE-2	OE-3
Fold expression	1.01	0.94	1.04	313.9	317.0	293.4

WT: BCG-WT (Tice)
OE: BCG-disA-OE (Tice)

Figure S1b

RAW Lucia ISG Reporter Assay
(IRF3 Induction Assay)

	NT-1	NT-2	NT-3	NT-4	WT-1	WT-2	WT-3	WT-4
ISRE (R.L.U.)	13114	11064	11560	12017	171552	159639	167460	170955

	OE-1	OE-2	OE-3	OE-4	LPS-1	LPS-2	LPS-3	LPS-4
ISRE (R.L.U.)	267912	263221	249400	277987	352021	349971	349409	330755

	c-di-AMP-1	c-di-AMP-2	c-di-AMP-3	c-di-AMP-4
ISRE (R.L.U.)	257169	257280	267583	273879

NT: No treatment
WT: BCG-WT (Pasteur)
OE: BCG-disA-OE (Pasteur)
LPS: LPS (E.coli)
c-di-AMP: Cyclic di-AMP

Figure S3b

% CD3+ of CD45 cells (MB49 Tumors)
Syngeneic MB49 heterotopic tumor model)
Flow Cytometry Analyses

Animal	C57BL/6 WT + Saline	STING$^{-/-}$ (C57BL/6J-Tmem173gt/J) + Saline	C57BL/6 WT + BCG-WT (Tice)	STING$^{-/-}$ (C57BL/6J-Tmem173gt/J) + BCG-WT (Tice)	C57BL/6 WT + BCG-*disA* -OE (Tice)	STING$^{-/-}$ (C57BL/6J-Tmem173gt/J) + BCG-*disA* -OE (Tice)
A1	13.7	6.9	42.2	16.0	42.7	64.1
A2	11.3	7.1	21.2	16.5	36.4	16.2
A3	19.5	6.3	25.0	13.5	73.6	6.36
A4	14.2	8.9	28.9	19.8	34.4	14.3
A5	13.6	6.8	30.6	15.8	70.5	36.0
A6	14.1	8.1	35.0	21.1	23.9	16.8

A: Animal

Figure S3c

% IFN-γ+ of CD8+ T cells (MB49 Tumors)
Syngeneic MB49 heterotopic tumor model)
Flow Cytometry Analyses

Animal	C57BL/6 WT + Saline	STING$^{-/-}$ (C57BL/6J-Tmem173gt/J) + Saline	C57BL/6 WT + BCG-WT (Tice)	STING$^{-/-}$ (C57BL/6J-Tmem173gt/J) + BCG-WT (Tice)	C57BL/6 WT + BCG-*disA*-OE (Tice)	STING$^{-/-}$ (C57BL/6J-Tmem173gt/J) + BCG-*disA*-OE (Tice)
A1	13.4	12.3	23.9	48.2	38.1	27.5
A2	13.3	21.3	19.7	33.0	39.8	20.3
A3	13.6	17.8	27.4	21.6	38.7	15.2
A4	11.9	13.7	35.0	37.7	32.3	13.8
A5	16.5	12.7	26.2	30.8	31.1	15.8
A6	17.6	22.9	31.9	26.8	40.0	27.3

A: Animal

Figure S3d

% CD69+CD38+ of CD8 T cells (MB49 Tumors)
Syngeneic MB49 heterotopic tumor model)
Flow Cytometry Analyses

Animal	C57BL/6 WT + Saline	STING$^{-/-}$ (C57BL/6J-Tmem173gt/J) + Saline	C57BL/6 WT + BCG-WT (Tice)	STING$^{-/-}$ (C57BL/6J-Tmem173gt/J) + BCG-WT (Tice)	C57BL/6 WT + BCG-*disA* -OE (Tice)	STING$^{-/-}$ (C57BL/6J-Tmem173gt/J) + BCG-*disA* -OE (Tice)
A1	10.1	10.5	42.5	26.3	52.9	29.3
A2	11.4	7.3	10.2	45.3	26.8	27.4
A3	23.3	8.1	34.3	9.0	55.7	16.1
A4	9.7	10.9	27.3	36.3	47.4	27.0
A5	15.4	11.9	31.6	14.0	58.9	43.3
A6	9.2	3.7	49.5	33.1	55.6	46.6

A: Animal

Figure S3e

	% TNF-α+ of CD206+ CD124+ cells (MB49 Tumors) Syngeneic MB49 heterotopic tumor model) Flow Cytometry Analyses					
Animal	**C57BL/6 WT + Saline**	**STING$^{-/-}$ (C57BL/6J-Tmem173gt/J) + Saline**	**C57BL/6 WT + BCG-WT (Tice)**	**STING$^{-/-}$ (C57BL/6J-Tmem173gt/J) + BCG-WT (Tice)**	**C57BL/6 WT + BCG-*disA* -OE (Tice)**	**STING$^{-/-}$ (C57BL/6J-Tmem173gt/J) + BCG-*disA* -OE (Tice)**
A1	13.5	6.6	27.9	19.4	21.0	20.4
A2	10.2	5.1	27.2	36.4	74.9	24.1
A3	13.2	6.8	39.2	14.6	57.1	10.4
A4	13.3	6.2	77.9	18.8	77.0	18.0
A5	15.1	5.6	100.0	18.6	59.4	18.9
A6	10.7	9.5	22.9	50.3	41.8	51.2

A: Animal

Figure S4a

Lung Bacillary Burden BALB/c Mice
D1 Implantation
Raw CFU per lung and log10 CFU per lung
(half of total lung homogenate plated on each of 2 plates).

CFU counts per plate (each animal lung plated in duplicate) (D1 implantation)				
Strain	**Plate 1**	**Plate 2**	**CFU (total)**	**Log10cfu**
BCG-WT (Tice)				
A1	53	57	110	2.045
A2	56	81	137	2.140
A3	66	99	165	2.220
BCG-*disA* -OE (Tice)				
A1	69	41	110	2.045
A2	253	142	395	2.598
A3	242	110	352	2.548

Figure S4b

Lung Bacillary Burden
(Day 28 Implantation in Balb/c Mice (Female))

	BCG-WT (Pasteur)	BCG-*disA* -OE (Pasteur)
Animal1	6.155	5.685
Animal2	6.083	5.621
Animal3	5.939	5.610
Animal4	6.162	5.976
Animal5	6.246	5.573

Figure S4c

Lung Bacillary Burden
(Day 1 Implantation in SCID Mice (Female)

	BCG-WT (Pasteur)	BCG-*disA* -OE (Pasteur)
Animal1	1.204	1.114
Animal2	1.146	0.954

Figure S4d (i)

Survival of SCID Mice infected with BCG
Time to Death Analyses

Days	BCG-WT (Pasteur)	BCG-*disA* -OE (Pasteur)	No treatment
60			
61			
62			
63			
64			
65			
66			
67			
68			
69			
70			
71			
72			
73			
74			
75			
76			
77			
78			
79			
80			
81			
82			
82			
83			
84	1		
85			
86			
87			
88			
89			
90			
91			
92	1		
92			
93	1		

Figure S4d (ii)

94			
95			
96			
97			
98		1	
98	1		
99	1		
100			
101			
102			
103			
104			
105			
106			
107			
108			
109			
110			
111			
112			
113			
114			
115			
116		1	
117			
118			
119			
120			
121			
122			
123			
124			
125			
126			
127			
128			
128			
128		1	
128	1		
129			
130	1		

Figure S4d (iii)

131			
131	1		
132			
133			
133			
133		1	
134		1	
134			
135	1		
136			
136			
136	1		
136		1	
137		1	
138			
139			
140			
141			
142			
143			
144			
145			
146			
147			
148			
149			
150			
151			
152			
153			
154			
155			
156			
157			
158			
159		1	
159			
160		1	
161			
162			
163			

Figure S4d (iv)

164			
165			
166			
167			
168		1	0
169			0
170			0
171			0
172			0
173			0
174			0
175			0
176			0
177			0

Figure S5

IFN-β q-PCR in resting and IFN-γ primed bone-marrow-derived macrophages

	NT-1	NT-2	NT-3
IFN-γ (-)	0.874	1.041	1.099
IFN-γ (+)	0.990	1.020	1.040

	WT (P)-1	WT (P)-2	WT (P)-3	OE (P)-1	OE (P)-2	OE (P)-3
IFN-γ (-)	1.855	1.857	1.635	5.861	5.413	4.671
IFN-γ (+)	1.922	0.872	1.371	12.804	16.244	10.175

	WT (T)-1	WT (T)-2	WT (T)-3	OE (T)-1	OE (T)-2	OE (T)-3
IFN-γ (-)	3.610	3.647	4.084	6.652	6.565	6.217
IFN-γ (+)	7.179	5.510	9.697	25.711	23.933	20.550

	LPS-1	LPS-2	LPS-3
IFN-γ (-)	44.494	41.608	42.005
IFN-γ (+)	585.049	547.881	570.034

NT: No treatment
WT (P): BCG-WT (Pasteur)
OE (P): BCG-disA-OE (Pasteur)
WT (T): BCG-WT (Tice)

Figure S11

Quantification lof LC3B-BCG colocalization in 5637 cells
MOI (20:1)

	WT (T)-1	WT (T)-2	WT (T)-3	OE (T)-1	OE (T)-2	OE (T)-3
% LC3B-BCG colocalization	10	5	12	25	28	35

WT (T): BCG-WT (Tice)
OE (T): BCG-disA-OE (Tice)

Figure S12b

GLUT1 expression on BMDMs after BCG infection (Flow cytomeric analyses)
MOI (20:1)

	NT-1	NT-2	WT (T)-1	WT (T)-2	OE (T)-1	OE (T)-2
Glut1+ macrophages	5.6	5.5	13.5	12.0	27.5	27.6

NT: No treatment
WT (T): BCG-WT (Tice)
OE (T): BCG-disA-OE (Tice)

Figure S12c

GLUT1 expression on BMDMs after BCG infection (Flow cytomeric analyses) MOI (20:1)

	NT-1	NT-2	WT (T)-1	WT (T)-2	OE (T)-1	OE (T)-2
2-NBDG Uptake (MFI)	355	360	420	415	491	510

NT: No treatment
WT (T): BCG-WT (Tice)
OE (T): BCG-disA-OE (Tice)